












Structural Applications of Ferritic Stainless Steels (SAFSS) WP2: Structural performance of steel members

Review of available data

Authors: Petr Hradil, Asko Talja, Esther Real, Enrique Mirambell

Confidentiality: Confidential until May 2014

Report's title SAFSS WP2: Review of available data					
Customer, contact person, address Commission of the European Communities		Order reference RFSR-CT-2010-00026			
Project name Structural Applications of Ferritic Stainless Steels		Project number/Short name 39594/SAFSS			
Author(s) Petr Hradil, Asko Talja, Esther Real, Enrique Mirambell		Pages 69 p.			
Keywords stainless steel, ferritic, finite element, review		Report identification code VTT-R-04651-12			
<p>Summary</p> <p>The report summarizes the experiences from previous research on stainless-steel structural members including the overview of experimental and numerical analyses and existing design methods and solutions of assessing the local, distortional and overall stability of thin-walled members. It is focused on the goals of Work Package 2 of SAFSS project and prepares the theoretical background for FE parametric studies, development of virtual testing tool and calibration tests.</p> <p>The aim of the document is to emphasize the effect of non-linear material behaviour typical for stainless steels and other metallic materials with focus on structural applications of ferritic grades. The behaviour of stainless steel in elevated temperatures is not included in the report as well as material anisotropy and corrosion resistance.</p> <p>Several recommendations and improvements of existing methods are proposed in the document as a result of thorough review of existing standards, background documentation, numerical and experimental investigations.</p>					
Confidentiality		Confidential until May 2014			
<p>Espoo 3.7.2012</p> <table border="0"> <tr> <td>Written by  Petr Hradil Research Scientist</td> <td>Reviewed by  Asko Talja Senior Research Scientist</td> <td>Accepted by  Eila Lehmus Technology Manager</td> </tr> </table>			Written by  Petr Hradil Research Scientist	Reviewed by  Asko Talja Senior Research Scientist	Accepted by  Eila Lehmus Technology Manager
Written by  Petr Hradil Research Scientist	Reviewed by  Asko Talja Senior Research Scientist	Accepted by  Eila Lehmus Technology Manager			
VTT's contact address P.O. Box 1000, FI-02044 VTT, Finland					
<p>Distribution (customer and VTT)</p> <table border="0"> <tr> <td>Project group VTT/Register Office</td> <td>1 pdf copy on project workspace 1 copy</td> </tr> </table>			Project group VTT/Register Office	1 pdf copy on project workspace 1 copy	
Project group VTT/Register Office	1 pdf copy on project workspace 1 copy				
<p><i>The use of the name of the VTT Technical Research Centre of Finland (VTT) in advertising or publication in part of this report is only permissible with written authorisation from the VTT Technical Research Centre of Finland.</i></p>					

Preface

This report is based on collected experimental and numerical data from Australia, South Africa, UK, Japan and other countries, and published theories to support design of ferritic stainless steel members. Scientific publications were systematically reviewed by VTT and UPC and compiled in such form that can serve as a basis for parametric FE modelling and member testing in WP 2 of SAFSS project.

The authors would like to thank Barbara Rossi from the University of Liège, Leroy Gardner from the Imperial College in London, and Nancy Baddoo from the Steel Construction Institute for valuable comments.

Espoo 3.7.2012

Authors

Contents

Preface	2
Abbreviations	5
1 Introduction	6
2 Tests on cold-formed stainless steel members.....	7
2.1 Test arrangements.....	7
2.2 Overview of experimental tests of stainless steel members.....	8
3 Web crippling.....	13
3.1 Introduction	13
3.2 Existing design rules	14
3.3 Existing research work.....	14
3.3.1 Carbon steel.....	14
3.3.2 Stainless steel.....	16
4 Design methods.....	23
4.1 The effective width method	23
4.2 The continuous strength method.....	25
4.3 The direct strength method	26
4.4 The Generalised Beam Theory (GBT)	27
4.5 The Erosion of Critical Bifurcation Load method (ECBL)	28
5 Solution schemes in FE analysis	29
5.1 Element selection.....	29
5.1.1 General purpose shell elements	29
5.1.2 Thin shell elements	29
5.1.3 Shell elements in Abaqus	30
5.1.4 Beam elements for the overall buckling behaviour.....	30
5.1.5 Mesh size.....	30
5.2 Geometric imperfections	30
5.3 Local buckling	31
5.4 Distortional buckling	31
5.5 Global (overall) buckling.....	32
6 Material models	33
6.1 Holmquist & Nadai model (1939)	33
6.2 Ramberg & Osgood model (1943)	33
6.3 Hill's modification (1944)	34
6.4 Mirambell & Real two-stage model (2000)	34
6.5 Rasmussen's modification (2003)	35
6.6 Gardner's modification (2006).....	35
6.7 Quach's three-stage model (2008).....	36
6.8 The generalized multi-stage model (2010).....	36
6.9 Models comparison	38
6.10 Explicit formulation of Ramberg-Osgood based models (2007– 2009) 40	
6.11 Generalized explicit formulation of multi-stage model (2010).....	41
6.12 Transformation for Abaqus solver	42
6.13 Overview of recommended material properties and designation .	42
6.14 Material models for FE applications	43

7	Enhanced strength of material.....	45
7.1	Enhanced corner properties.....	45
7.2	Corner extensions.....	46
7.3	Enhanced cold-rolled faces properties.....	46
7.4	Average yield strength	47
8	Residual stresses	48
8.1	Bending residual stresses	48
8.2	Axial (membrane) residual stresses.....	49
9	Strength curves	50
9.1	Ayrton-Perry curve (1886).....	50
9.2	Nonlinear material	53
9.2.1	Transformation of Euler's curve	53
9.2.2	Transformation of Ayrton-Perry curve	55
10	Numerical studies overview	58
	References	61

Abbreviations

AS/NZS	Australian Standard/New Zealand Standard
BS	British Standard
CC	Concentric compression
CEN	European Committee for Standardization
CHS	Circular hollow section
CRF	Circle-to-rectangle forming
CSM	Continuous Strength Method
DSM	Direct Strength Method
EC	Eccentric compression
EOF, ETF	End one-flange loading, End two-flange loading
EN	European standards
FB	Flexural buckling
FE, FEA	Finite element, Finite element analysis
FEM	Finite element method
FSM	Finite strip method
GBT	Generalized beam theory
GMNIA	Geometrically and materially nonlinear analysis with imperfections
GUI	Graphic user interface
IOF, ITF	Interior one-flange loading, Interior two-flange loading
LEA (LBA)	Linear eigenvalue (buckling) analysis
LTB	Lateral-torsional buckling
OHS	Oval hollow section
RHS	Rectangular hollow section
Riks	Arc-length method used e.g. in Abaqus FE solver
SEI/ASCE	Structural Engineering Institute/American Society of Civil Engineers
SHS	Square hollow section
TB, TFB	Torsional buckling, Torsional-flexural buckling
UNS	Unified Numbering System for Metals and Alloys

1 Introduction

The report summarizes the experiences from previous research on stainless-steel structural members including the overview of experimental and numerical analyses and existing design methods and solutions of assessing the local, distortional and overall stability of thin-walled members. It is focused on the goals of Work Package 2 of SAFSS project and prepares the theoretical background for FE parametric studies, development of virtual testing tool and calibration tests.

The aim of the document is to emphasize the effect of non-linear material behaviour typical for stainless steels and other metallic materials with focus on structural applications of ferritic grades. The behaviour of stainless steel in elevated temperatures is not included in the report as well as material anisotropy and corrosion resistance.

Several recommendations and improvements of existing methods are proposed in the document as a result of thorough review of existing standards, background documentation, numerical and experimental investigations.

2 Tests on cold-formed stainless steel members

Due to the nonlinear material behaviour, complex residual stresses distribution and variability of material strength over the work-hardened member cross-section, experiments are important means of verification of analytical or numerical calculations of cold-formed stainless steel members. The chapter briefly summarizes more than 500 member tests performed in selected research institutes during last two decades.

2.1 Test arrangements

Stub column test

Stub column test is mostly used to evaluate the effects of local and distortional buckling. According to Eurocode 3, Part 1-3 [1] the specimen should have length at least 3 times the maximum plate element width and smaller than 20 times radius of gyration.

Member buckling test

In order to determine effect of overall buckling, compression tests are usually needed on members with different effective length. Eurocode 3, Part 1-3 [1] recommends to perform at least 5 test for each of the following slenderness: 0.2; 0.5; 0.7; 1.0; 1.3; 1.6; 2.0; 3.0.

Usually the experiment configuration simulates pinned ends that allows for lower overall critical load and shorter members [2–6]. However, the fixed end-conditions are also presented in some studies [7–9] by extending the stub column tests to the overall buckling failure lengths. The most frequent type of member buckling test is concentric compression (CC), where the load is positioned in the centre of gravity of the cross-section. The concentric test results usually shows very good agreement with numerical simulations if the FEM model contains the same amplitude of geometric imperfections as measured on the real member. The best results can be achieved by perturbing the model with the real distribution of geometric imperfections, material strength and residual stresses. Several studies included also eccentric compression tests (EC), where the eccentricity of load simulates the assumed geometrical imperfections in design codes ($L/1000$ [3] or $L/1500$ [6]). Geometric imperfections are discussed also in Chapter 5.2.

Bending test

Four-point bending test or three-point bending test is usually recommended to evaluate the bending capacity of full cross-section or the lateral-torsional stability in bending. In case of four-point bending test, the loads should be applied at 0.2 to $0.33 L$ from the ends of member.

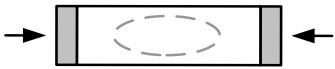
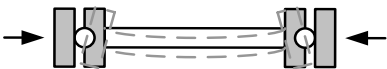
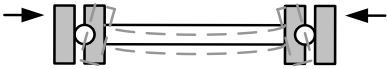
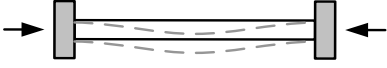
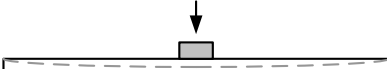
Web-crippling tests

Web crippling tests are discussed in more detail in Chapter 0.

2.2 Overview of experimental tests of stainless steel members

The following overview (Table 1) includes collected references about stainless steel experimental tests and is focused especially on member tests such as stub column, flexural buckling, bending or web crippling experiments. Short notes about test specimen, material and loading are given in the Table 2 and Table 5.

Table 1. General overview of experimental tests.

Test arrangement	Austenitic	Duplex	Ferritic
 <p>Stub column test (Local/distortional buckling test)</p>	Rasmussen and Hancock (1993) Talja and Salmi (1995) Talja (2000) (Eur Com) Young and Hartono (2002) Kuwamura (2003) Young and Liu (2003) Gardner and Nethercot (2004) Talja (2004) (Eur Com) Young and Liu (2005) Gardner et al. (2006) Mcdonald et al. (2007) Jandera et al. (2008) Becque and Rasmussen (2009)	Talja (2000) (Eur Com) Rasmussen et al. (2003) Young and Liu (2006) Bardi and Kyriakides (2006) Theofanous and Gardner (2009)	Rossi et al. (2010) Lecce and Rasmussen (2006) Becque and Rasmussen (2009)
 <p>Member buckling test concentric (CC)</p>	Rasmussen and Hancock (1993) Talja and Salmi (1995) Talja (2000) (Eur Com) Gardner and Nethercot (2004) Talja (2004) (Eur Com) Gardner et al. (2006) Mcdonald et al. (2007) Becque and Rasmussen (2009)	Zhou and Young (2005) Theofanous and Gardner (2009)	Bredenkamp and van den Berg (1995) Becque and Rasmussen (2009)
 <p>Member buckling test eccentric (EC)</p>	Rasmussen and Hancock (1993) Talja and Salmi (1995) Talja (2000) (Eur Com) Talja (2004) (Eur Com) Mcdonald et al. (2007) Becque and Rasmussen (2009)		Becque and Rasmussen (2009)
 <p>Member buckling test with fixed ends</p>	Young and Hartono (2002) Young and Liu (2003) Liu and Young (2003)		Rossi et al. (2010)
 <p>3-point bending tests</p>	Mirambell and Real (2000) Gardner and Nethercot (2004) Gardner et al. (2006)	Theofanous and Gardner (2010)	

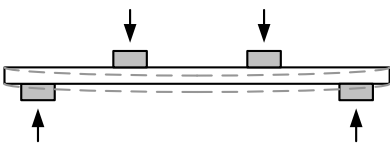
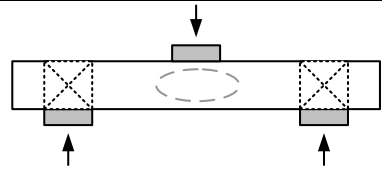
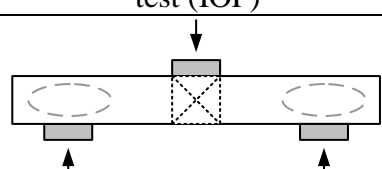
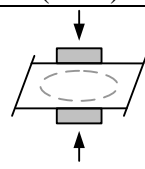
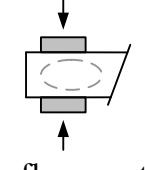
Test arrangement	Austenitic	Duplex	Ferritic
 <p>4-point bending tests</p>	Rasmussen and Hancock (1993) Talja and Salmi (1995) Talja (2000) (Eur Com) Young (2003) Talja (2004) (Eur Com) Zilli (2004) (Eur Com) Zhou and Young (2005)	Talja (2000) (Eur Com) Burgan (2000) (Eur Com) Zhou and Young (2005)	
 <p>One-flange interior web crippling (internal support) test (IOF)</p>	Korvink et al. (1995) Talja and Salmi (1995) Talja (2004) (Eur Com) Zilli (2004) (Eur Com) Gardner and Nethercot (2004b) Gardner et al. (2006) Zhou and Young (2007)	Zhou and Young (2007)	Korvink et al. (1995)
 <p>One-flange exterior web-crippling (end support) test (EOF)</p>	Korvink et al. (1995) Zhou and Young (2007)	Zhou and Young (2007)	Korvink et al. (1995)
 <p>Two-flange interior web crippling test (ITF)</p>	Korvink et al. (1995) Sélen (1999) (Eur Com)		Korvink et al. (1995)
 <p>Two-flange exterior web crippling test (ETF)</p>	Korvink et al. (1995) Sélen (1999) (Eur Com)		Korvink et al. (1995)

Table 2. Detailed overview of experimental tests.

Centro Sviluppo Materiali S.p.A. (2004) Zilli & Fattorini [10]	
Material	1.4318 (austenitic)
Sections	trapezoidal sheeting
Loading	bending test, internal support test
Czech Technical University in Prague Jandera et al. (2008) [11]	
Material	1.4301 (type 304 austenitic)
Sections	SHS 60x60, 80x80, 100x100, 120x120 (thickness 2 and 4 mm)
Loading	stub column test
No. of tests	16
Glasgow Caledonian University Mcdonald and Rhodes (2007) [5]	
Material	1.4301 (type 304 austenitic)
Sections	lipped channels
Loading	concentric (CC) and eccentric (EC 4 to 16 mm) flexural buckling tests stub column test, flexural buckling test (with 4–16 mm eccentricity)
No. of tests	22 (CC, 2005), 22 (EC 8 mm, 2005), 28 (EC 4 to 16 mm, 2007)
Imperial College Gardner and Nethercot (2004) [4, 12, 13] Theofanous and Gardner (2006–2010) [14–16]	
Material	1.4301 (type 304 austenitic for SHS, RHS and CHS) 1.4401 (type 316 austenitic for OHS) 1.4318 (for SHS, RHS) 1.4162 (lean duplex for SHS, RHS)
Sections	SHS 60x60 to 150x150 (thickness 2 to 8 mm, 40 tests), RHS 60x40 to 150x100 (thickness 2 to 6 mm, 40 tests), CHS 101.6 to 153 (thickness 1.5 to 4 mm, more than 4 tests) OHS 121x76, 86x58 (thickness 2 and 3 mm, 20 tests)
Loading	stub column test (51 tests), flexural buckling (30 tests), 3-point bending (23 tests)
No. of tests	more than 104
Luleå University of Technology Sélen et al. (2000) [17] (EurCom)	
Material	1.4301 (type 304 austenitic)
Sections	welded I
Loading	web crippling test (patch loading and end-patch loading)
No. of tests	9
Rand Afrikaans University (University of Johannesburg) Korvink et al. (1995) [18] Bredenkamp et al. (1995) [19]	
Material	type 304 (austenitic), type 430 (1.4016 ferritic), modified type 409 (titanium stabilised 3Cr12 ferritic)
Sections	lipped channel (double lips-facing), welded I sections
Loading	web crippling test (see Chapter 0), flexural buckling test

Steel Construction Institute	
Burgan et al. (2000) [17] (EurCom)	
Material	1.4301 (austenitic), 1.4462 (duplex)
Sections	CHS
Loading	bending
No. of tests	8
University of Hong Kong	
Young and Hartono (2002) [7]	
Liu and Young (2003) [9]	
Young and Liu (2003) [8]	
Zhou and Young (2005–2008) [20–25]	
Material	type 304 (austenitic), HAS high strength austenitic, 1.4462 (duplex)
Sections	CHS 89x3, 169x3.5, 323x4.5 (16 tests) SHS 40x40–80x80 (thickness 2 or 5 mm, more than 12 tests) RHS 40x120, 50x100, 60x120, 80x120 (thickness 2 to 6 mm, over 24 tests)
Loading	stub column test (CHS: 3 tests, RHS: 8 tests), flexural buckling test with fixed ends (CHS: 13 tests, SHS: 12 tests, RHS: 16 tests), web-crippling
No. of tests	52 (2002–2003), more than 91 (2005–2007), 21 (2008)
University of Liège (2010)	
Rossi et al. [26]	
Material	1.4003 (3Cr12 ferritic)
Sections	lipped channel
Loading	stub column distortional buckling test, combined distortional and flexural-torsional buckling test, flexural-torsional buckling test
No. of tests	30
Universitat Politècnica de Catalunya	
Mirambell and Real (2000) [27]	
Material	type 304 (austenitic)
Sections	SHS 80x80 (thickness 3 mm, 4 tests) RHS 80x120 (thickness 4 mm, 4 tests) H 100x100 (thickness 8 mm, 4 tests)
Loading	3-point bending on simply supported and continuous beams
No. of tests	12
University of Sydney	
Rasmussen and Hancock (1993) [2, 28], Burns and Bezkorovainy (2001) [29], Becque and Rasmussen (2009) [6, 30]	
Material	type 304 (austenitic), type 430 (austenitic), 3cr12 (ferritic), type 404 (ferritic), 1.4462 (duplex for plate buckling tests)
Sections	1993: SHS 25-80x3, RHS 51-84x25-38x3, CHS 33.4-101.5x2.85-3.2 2006: lipped channels, double lipped channels (bolted I sections)
Loading	stub column test, 4-point bending test (SHS 80x3 and CHS 101.5x2.85), flexural buckling test concentric (CC) and eccentric (EC, L/1500)
University of Texas	
Bardi & Kyriakides (2006) [31]	
Material	1.4410 (duplex)

Sections	CHS
Loading	stub column test
No. of tests	18
University of Tokyo Kuwamura (2001)	
Material	1.4301, 1.4318 (originally SUS304 type 304 austenitic, SUS301L 3/4H)
Sections	cold-formed – angles (12 tests), channels (11 tests), lipped channels (12 tests), CHS (10 tests), laser-welded – I sections (16 tests), square sections (12 tests)
No. of tests	73
VTT Technical Research Centre of Finland (1995) Talja and Salmi (1995) [3], Talja (2000) [17] (EurCom), Talja (2004) [10] (EurCom)	
Material	1995: 1.4301 (type 304 austenitic) 2000: 1.4541 (type 321 austenitic), 1.4435 (austenitic) 2004: 1.4318 (austenitic), 1.4571 (austenitic)
Sections	1995: SHS 60x5, RHS 150x100x3, RHS 150x100x6 2000: CHS 140x4 (1.4541), 140x3 and 140x2 (both 1.4435) 2004: SHS 100x3, SHS 80x3 (only flexural buckling test), RHS 120x80x3, 140x60x3, Channel C-150x75x30x2.7-4, Z section Z-150x75x30x2.7-4 (only bending test), trapezoidal sheeting, top hat profiles
Loading	1995: stub column test (3 tests), flexural buckling concentric (CC, 9 tests), and eccentric (EC, ecc. L/1000, 12 tests), 4-point bending (9 tests), web-crippling (IOF, 6 tests, see Chapter 0) 2000: stub column test (3 tests), flexural buckling concentric (CC, 6 tests) and eccentric (EC, 8 tests) 2004: bending test, internal support test, flexural buckling test, stub column test
No. of tests	more than 56

3 Web crippling

3.1 Introduction

Cold-formed structural members are really useful due to their high strength-to-weight ratio compared with other structural materials. They are usually members with high width-to-thickness and high height-to-thickness ratios so the designer has to focus more thoroughly on the instability phenomena: web buckling, web crippling, buckling due to shear, etc.

Web crippling is a form of localized buckling that occurs in a cold-formed steel section at points of concentrated loads or supports where stresses are excessive.

Depending on the section and its dimensions web buckling, web crippling and often a combination of both can occur, even when loads are not transferred evenly into webs. This condition can reduce the load carrying capacity of flexural members as the bearing capacity is governed by the web crippling resistance.

The theoretical analysis of web crippling under concentrated loading condition is very complex because it involves a large number of factors, such as the non-uniform stress distribution, initial imperfection of the web plate, local yielding in the region of load application, elastic and inelastic instability of the web plate, and other factors according to Yu (2000). Due to these difficulties, most of the research carried out mainly in carbon steel and therefore predictions, as well as recommendations, have been based on experimental results. Hence, the web crippling design equations are empiric.

The main problem of these recommendations is that are confined to the range for which they have been proved and do not give adequate insight in the structural behavior. Furthermore, these expressions for stainless steel have been extrapolated from carbon steel without taking into account differences between both materials.

In general, current design rules provide empirically defined formulae for the calculation of web crippling strength of cold-formed steel members. Four different loading conditions can generally be distinguished:

- EOF = End One-Flange loading
- IOF = Interior One-Flange loading
- ETF = End Two-Flange loading
- ITF = Interior Two-Flange loading.

If the distance between the edges of the bearing plates on opposite sides of the web is more than 1.5 times the web height h_w , one-flange loading is assumed to govern. If the distance is less than 1.5 times the web height, two-flange loading is assumed. Moreover, if the distance from the end of the member to the outer edge of the bearing or support plate is less than 1.5 times the web height, the loading is assumed to be end loading. If the distance is more than 1.5 times the web height, interior loading is assumed [32].

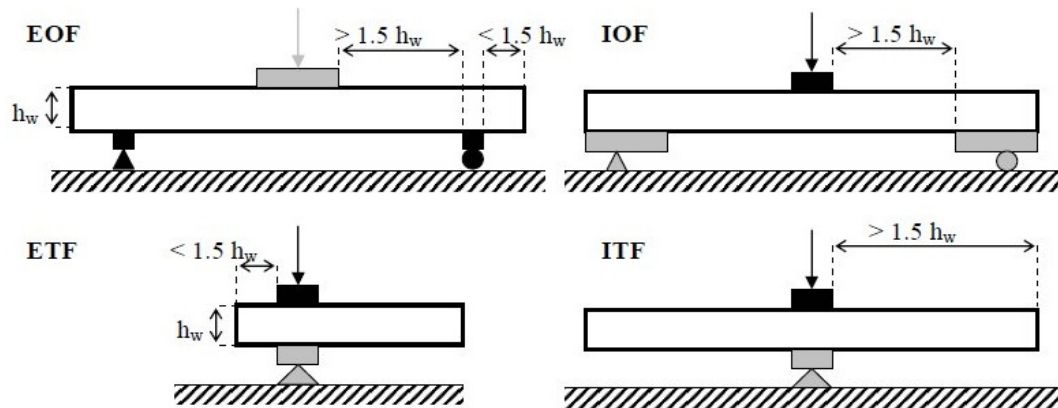


Figure 1.

The calculation of web crippling load tends to be a cumbersome design procedure. To assist designers it is therefore necessary to develop equations that provide a reasonably fast and efficient web crippling check.

3.2 Existing design rules

The web crippling design rules in specifications for stainless steel structures are adopted from the specifications for carbon steel structures. The web crippling design rules for stainless steel can be found in EN 1993-1-4 [33] for stainless steel members, referred to the EN 1993-1-3 [1] for steel cold formed members.

Other specifications for the design of cold-formed stainless steel structural members are the American Society of Civil Engineers Specification [34] and the Australian/New Zealand Standard [35].

The web crippling design rules in these specifications are generally classified into the four loading conditions, namely, end-one-flange (EOF), interior-one-flange (IOF), end-two-flange (ETF), and interior-two-flange (ITF). In addition, the American Design Standard specification (NAS, 2004) proposes an integrated formula which involves the four load cases.

3.3 Existing research work

3.3.1 Carbon steel

Because of the many factors influencing the ultimate web crippling strength of cold-formed steel sections, the majority of research has been experimental, but also finite element modeling has been used to model web crippling behavior. Some authors have also created so-called mechanical models for web crippling [36, 37].

The current design methods are based on curve-fitting of experimental results, which has been criticized for two main reasons [38]: "(i) the rules are strictly confined to the range for which they have been proven, and (ii) it is often difficult to ascertain the engineering reasoning behind the different parts of the rather complex equations". The same criticism has been made by Hofmeyer [37]. For these reasons, a number of researchers have worked to create mechanical models that could be used to produce more accurate and descriptive design methods for web crippling. Although promising results have been achieved, especially at the

University of Eindhoven in the Netherlands [36, 37], these methods have not yet been incorporated in design practice [32].

A great amount studies involving web crippling strength of carbon steel have been carried out. The first research on web crippling was conducted in Cornell University by Winter and Pian in 1946 [39]. They first identified the four load cases used in web crippling studies. Based on their tests, Winter and Pian found that the web crippling strength of unreinforced webs depends primarily on the yield strength of the steel and on the geometric ratios of sections which are still used in current web crippling equations. Since then, several researchers have carried out comprehensive experimental studies on interior loading [40–43] and End One-Flange loading of multi-web deck sections [41–45] and the interaction of bending and web crippling of multi- web deck sections [44–46]. Experimental studies on web crippling of high strength steel beams under the four load conditions and involving channel sections and hollow sections were also performed by Santaputra et al. [47], Young and Hancock [48] and Zhao and Hancock [49].

Some researchers have also proposed so-called mechanical models as an alternative method for the web crippling study. These mechanical models are based on mechanics rather than curve fitting of experimental results and describe the behaviour of sections.

Bähr [50] developed an analytical model for the prediction of ultimate load for sheeting under pure concentrated load at an end support. Bakker [36] used the yield line theory to create a numerical model to simulate web crippling of a cold formed steel hat section where he aimed to reduce the statistical deviation between experimental data and theoretical load capacity instead of design equations. Reinsch [51] developed a mechanical model to determine the failure load of sheeting taking into account the moment redistribution. Tsai and Crisinel [52] developed a mechanical model for the prediction of ultimate load of sheeting. Vaessen [53] developed two different models for the prediction of the ratio between force and web crippling deformation. Hofmeyer [37] developed post-failure mechanical models covering all post-failure modes.

Nowadays, the research work is focused on the determination of the failure mechanical models based on the yield line theory, to create a simplified and generalised expression for the web crippling strength of cold-worked sections. Three different mechanical models, depending on the problem and cross-section geometry, can be distinguished according to Bakker [36] and Hofmeyer [37]:

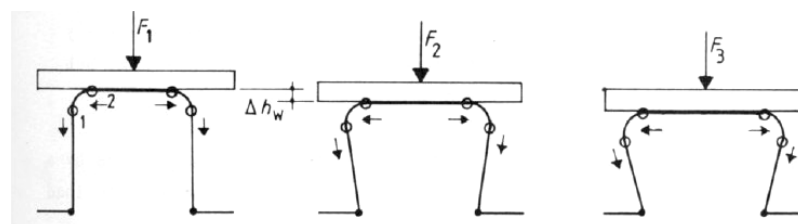


Figure 2. The rolling mechanism.

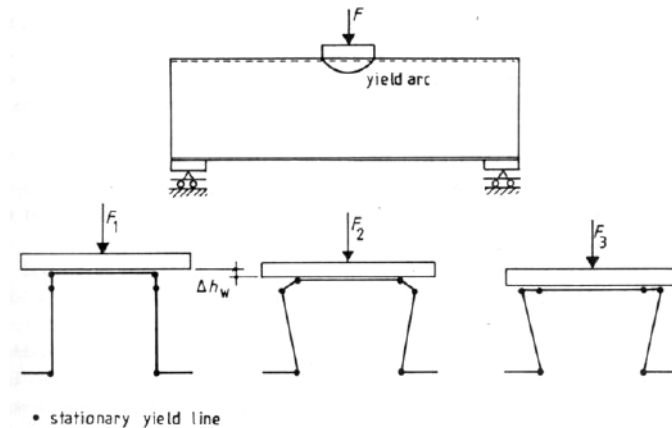


Figure 3. The yield arc mechanism.

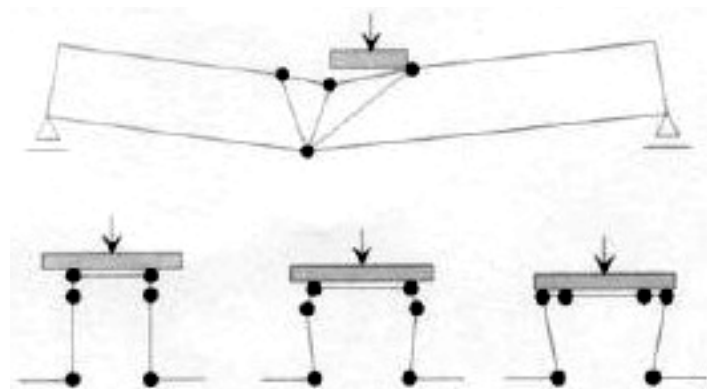


Figure 4. The yield eye mechanism.

The rolling mechanism is dominant when sections are subjected to large concentrate loads and small bending moments. However, in practice sections are subjected to both large concentrate loads and large bending moments. In these cases the most dominant mechanisms are the yield arc and the yield eye mechanisms.

Hofmeyer [54] developed a new model which insight the structural behavior of steel sections based on two existing models. This model has been compared to experimental data carried out by Wing [46] and Hofmeyer [55], and also to Eurocode 3 [1].

Hofmeyer also worked on the behaviour of hat steel sections in [56] and checked whether the cross-sectional behaviour (location and movement of yield lines) can be described by 2D finite element models (strips). The conclusions showed that for small corner radii the behavior of the whole section and 2D stripes is equal but not for large radii. However, the first yield line movement and location is equal for all corner radii so it is possible to investigate the total section by only using a 2D strip.

3.3.2 Stainless steel

A lack of studies involving web crippling strength of stainless steel comparing with carbon steel can be noticed. A table at the end of this chapter summarizes research on web crippling of cold-formed stainless steel sections.

The first web crippling studies carried out in stainless steel found in the literature were performed by Korvink et al. [18] in the Rand Afrikaans University. The objective of this study was to compare experimental results on stainless steel lipped channel sections subjected to web crippling with the 1991 ASCE Specification for the Design of Cold-Formed Stainless Steel Structural Members [34] which is based on the Specification for the Design of Cold-Formed Steel Structural Members with Commentary [57] for carbon steel. The stainless steel grades used were AISI 304, 430 and 409 (or 3Cr12).

Other experimental investigations were carried out by Talja and Salmi (1995). Their test programme included also 6 support reaction experiments (EOF) on 3 different RHS sections from AISI 304 (1.4301) stainless steel.

New studies on web crippling were developed later in 2004 for a new European project, specifically devoted to structural design of cold worked austenitic stainless steel members. Talja and Zilli [10] fulfilled studies on stainless steel type 1.4318 in two conditions: annealed with similar to strength level C700 with 330–350 MPa and cold worked with a strength level C850. The tests were performed under IOF loading. The former tested RHS which dimensions were 100x100x3 120x80x3 140x60x3 with two specimens for each section size for C700 and C850 so a total of 6 tests were performed. The latter carried out 8 test on trapezoidal unstiffened profiles, 3 tests on trapezoidal stiffened profiles and 9 tests on top hat profiles. The objective of Talja and Zilli was to study the behavior of aforementioned sections comparing experimental and numerical simulations with EN 1993-1-4 [33].

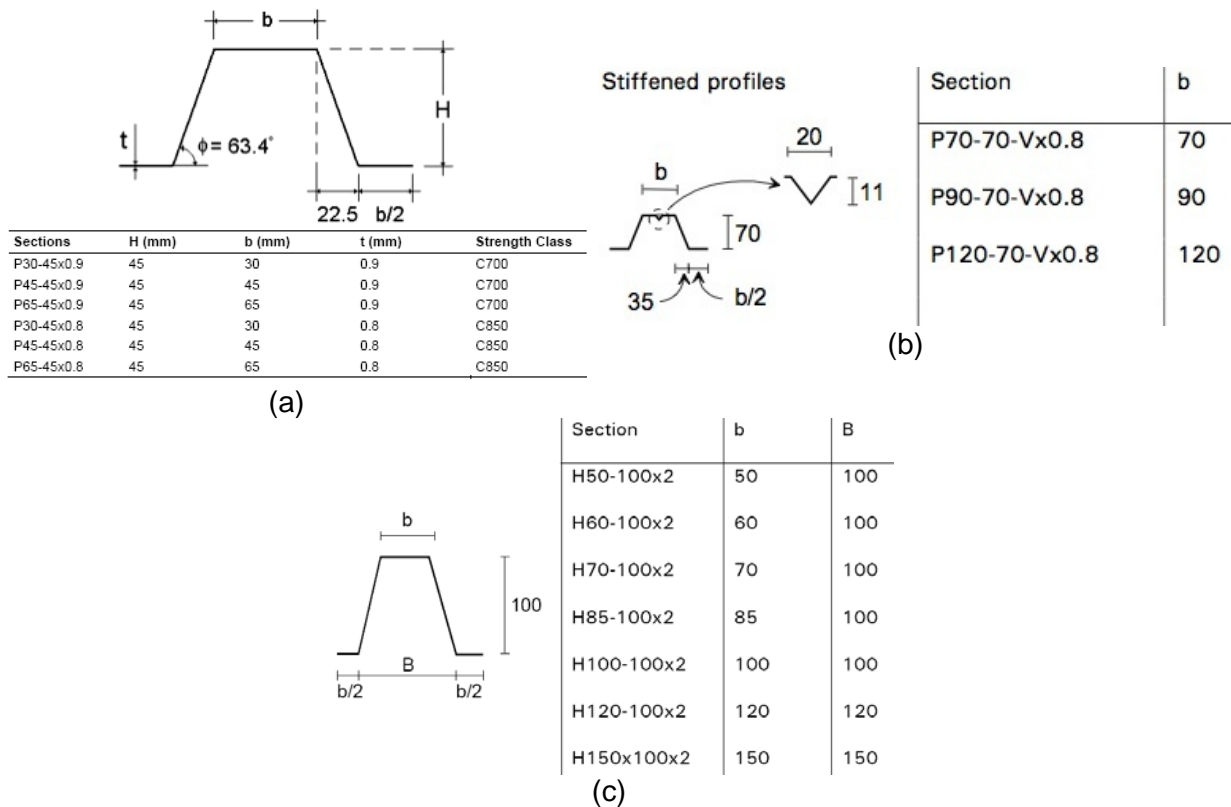


Figure 5. (a) Unstiffened trapezoidal profile; (b) Target dimensions of stiffened trapezoidal profile; (c) Target dimensions of hat sections founded in Zilli (2004) [30].

Since 2006, Zhou and Young have been carrying out amount of tests on cold formed stainless steel members subjected to web crippling. Tests of cold-formed stainless steel square and rectangular hollow sections are described by Zhou and Young [20] for normal strength materials and by Zhou and Young [23] for high strength materials. A total of 91 tests were performed under the four IOF, EOF, ITF and ETF loading conditions. In these studies the unified equation (1) in the NAS specification for cold-formed carbon steel is adapted to different stainless steel grades. The coefficients proposed are shown in the next table:

$$P_p = Ct^2 f_y \sin \theta \left(1 - C_R \sqrt{\frac{r_i}{t}} \right) \left(1 + C_N \sqrt{\frac{N}{t}} \right) \left(1 - C_h \sqrt{\frac{h}{t}} \right) \quad (1)$$

Table 3. Proposed web crippling design parameters for cold-formed stainless steel square and rectangular hollow sections calibrated in Zhou and Young (2006a) and Zhou and Young (2007a).

Support and flange conditions		Load condition	C	C _R	C _N	C _h	LRFD ϕ_w	Limits		Type
								h/t	N/h	
Unfastened	Stiffened or Partially Stiffened	ETF	3.0	0.40	0.60	0.001	0.80	≤ 60	≤ 2.0	304
		ITF	6.0	0.26	0.48	0.001	0.70	≤ 60	≤ 2.0	
	Flanges	EOF	5.0	0.40	0.50	0.020	0.70	≤ 50	≤ 2.0	HSA
		IOF	7.0	0.21	0.26	0.001	0.70	≤ 50	≤ 2.0	and Duplex
		ETF	3.0	0.36	0.50	0.020	0.80	≤ 50	≤ 2.0	
		ITF	7.0	0.11	0.24	0.001	0.70	≤ 50	≤ 2.0	
Unfastened	Stiffened or Partially Stiffened	EL	5.6	0.25	0.28	0.001	0.80	≤ 200	≤ 2.0	304
		IL	12.2	0.24	0.18	0.001	0.80	≤ 200	≤ 2.0	
	Flanges	EL	5.8	0.26	0.18	0.001	0.80	≤ 200	≤ 1.6	HSA
		IL	15.3	0.26	0.08	0.003	0.80	≤ 200	≤ 1.6	and Duplex

Notes: The above coefficients apply when $N/t \leq 50$, $r_i/t \leq 2.0$ and $\theta = 90^\circ$.

HSA = High Strength Austenitic

Using the tests, Zhou and Young [58] proposed a new design procedure derived through a combination of theoretical and empirical analysis for cold formed stainless steel RHS, SHS sections under web crippling. Three yield line mechanisms models were developed, one for end loading (EL) condition while the others for the interior two-flange loading (ITF) condition and the exterior two-flange loading (ETF) condition.

Furthermore, Zhou and Young [21] performed 64 tests on stainless steel SHS and RHS seated on a solid foundation subjected to web crippling IF and EF loading which is not include in the design rules. The stainless steel grades were high strength 304 and duplex. The main objective of the study was to calibrate the coefficients of the unified equation of NAS specification for this particular case. The next figure shows a schematic view of test arrangement and the calibrated coefficients of unified NAS equation.

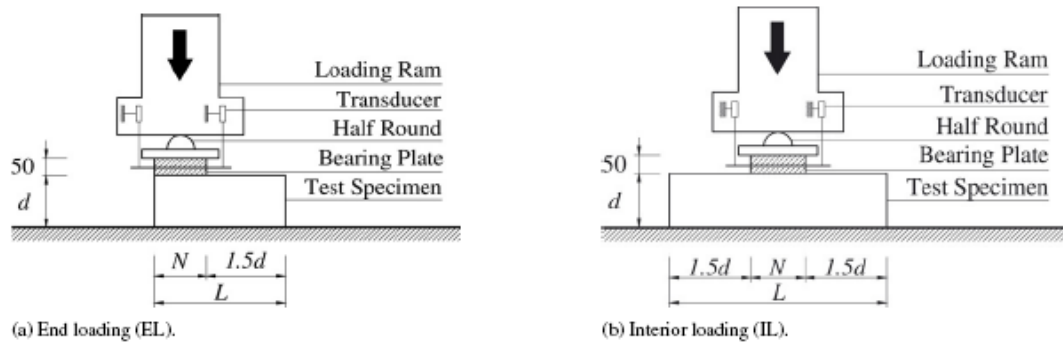


Figure 6. Schematic view of test arrangements and calibrated coefficients in Zhou & Young (2007b) [34].

Table 4. Proposed web-crippling design rules for cold-formed stainless steel hollow sections.

Support and flange conditions		Load cases	C	C_R	C_N	C_h	LRFD ϕ_w	Type
Unfastened	Stiffened or partially stiffened flange	End loading (EL)	5.6	0.25	0.28	0.001	0.80	304 HSA, and duplex
		Interior loading (IL)	12.2	0.24	0.18	0.001	0.80	
		End loading (EL)	5.8	0.26	0.18	0.001	0.80	
		Interior loading (IL)	15.3	0.26	0.08	0.003	0.80	

Notes: The above coefficients apply when $h/t \leq 200$, $N/t \leq 140$, $N/h \leq 2.0$, $r_f/t \leq 9.5$ and $\theta = 90^\circ$. HSA = High Strength Austenitic.

Moreover, an experimental investigation on cold-formed stainless steel SHS and RHS subjected to combined bending and web crippling was also carried out by Zhou and Young [22], and a total of 21 tests were conducted. The objective of the authors was compared experimental results with strengths obtained using design rules.

A review of all studies dealing with web crippling of cold-formed stainless steel tubular sections performed by Zhou and Young can be founded in Zhou and Young [24].

Table 5. Detailed overview of web-crippling studies.

Korvink et al. [18]	
Rand Afrikaans University (University of Johannesburg 1995)	
Material	type 304 (austenitic), type 430 (1.4016 ferritic) , modified type 409 (titanium stabilised 3Cr12 ferritic), HSSy normal
Sections	lipped channel (double lips-facing) by press braking process
Loading	EOF
Objective	To validate the 1991 ASCE for cold-formed stainless steel and based on 1986 AISI for cold-formed carbon steel using experimental results (Pe). 139 tests
Specifications and methods involved	<ul style="list-style-type: none"> - The 1991 ASCE Specification for the Design of Cold-Formed Stainless Steel Structural Members. - 1986 AISI Specification for the Design of Cold-Formed Steel Structural Members with Commentary.
Conclusions and remarkable observations	<ul style="list-style-type: none"> - Two failure mechanisms are observed without a clear transition: bearing failure or overstressing under the bearing plates (smaller channel sections); global buckling (larger web heights). - Ratio P_e/P_t calculated using ANSI/ASCE-8-90 is not always

	<p>acceptable (a value of 1.0 or within 20% Thereof), except the values obtained for stainless steel Type 430.</p> <ul style="list-style-type: none"> - The web crippling loads tend to be less conservative with an increase in web slenderness ratio or bearing length. - Using transverse compression yield strength instead of longitudinal compression yield strength as 1991 ASCE recommends better values were obtained.
Talja & Salmi [3] VTT, Technical Research Centre of Finland (1995)	
Material	type 304 (austenitic)
Sections	SHS 60x60 (formed from circular tube, thickness 5 mm), RHS 100x150 (cold-rolled, thickness 3 and 6 mm)
Loading	IOF
Objective	To evaluate the current European and American design rules. To compare results with those obtained using a) elastic bending resistance b) plastic bending resistance c) “real” moment capacity from bending tests.
Specifications and methods involved	ENV 1993-1-3 (1993), Annex S ANSI/ASCE-8-90 (1991)
Conclusions and remarkable observations	<ul style="list-style-type: none"> - The results of web crippling satisfy the condition given in Eurocode 3 and ANSI/ASCE specifications. - The results indicate that higher design strength than R_{p02} could be used but then all the rules concerning flexural buckling, plate buckling, plastic design, etc. have to be verified thoroughly.
Talja et al. [10] VTT, Technical Research Centre of Finland (2004)	
Material	1.4318 or X2CrNi18-7 in two conditions: Annealed (similar to strength level C700 with 330–350 N/mm ²) Cold worked (strength level C850)
Sections	RHS: 100x100x3 120x80x3 140x60x3 with two specimens for each section size for C700 and C850
Loading	IOF
Objective	To compare experimental and numerical results (using ABAQUS, S9R5 without residual stress but considering local imperfections) with design rules. 6 tests
Specifications and methods involved	<ul style="list-style-type: none"> - EC3 Part 1-4 that refers to EC3 Part 1-3 - The deformation capacity based design method but it has not been developed to cover web crippling so only EC3 Part 1-3 was compared.
Conclusions and remarkable observations	<ul style="list-style-type: none"> - The comparison with EC3 1-3 shows that EC predicts, on average, 83% of the failure load for web crippling, with a relatively small scatter. These results are approximately in the same line with those calculated for standard-strength material. - Extension of EC3 to the high strength grades has been recommended.
Zilli & Fattorini [10] Centro Sviluppo Materiali S.p.A. (2004)	
Material	1.4318 or X2CrNi18-7 in two conditions:

	Annealed (similar to strength level C700 with 330–350 N/mm ²) Cold worked (strength level C850)
Sections	Trapezoidal unstiffened profiles (8 tests) Trapezoidal stiffened profiles (3 tests) Top hat profiles (9 tests) H50 x100x2, H100 x100x2 and H150x100x2
Loading	IOF
Objective	To study the behaviour of cold-formed open sections and sheeting comparing between numerical (ABAQUS) and experimental analysis and compare between existing guidance and exp/numerical studies
Specifications and methods involved	EC3 Part 1-4 that refers to EC3 Part 1-3
Conclusions and remarkable observations	<ul style="list-style-type: none"> - EN 1993-1-3 is conservative for unstiffened trapezoidal profiles. In addition, the results indicate that there is scope for improvement in the design interaction equation. - EN 1993-1-3 is conservative for top hat profiles and that the design interaction equation can be modified to yield a better fit to the experimental and FE results. - EN 1993-1-3 is conservative for stiffened trapezoidal profiles and, again, the design interaction equation can be modified to yield a better fit to the experimental results.
Zhou & Young [20, 23] University of Hong Kong (2006–2007)	
Material	304 Normal strength (2006), High strength (2007), Duplex (2007)
Sections	SHS, RHS (8 sections in 2006), SHS, RHS (7 sections in 2007) 91 tests in total
Loading	IOF, EOF, ETF, ITF
Objective	To compare experimental results (PEXP) with design strength (Pn)
Specifications and methods involved	<ul style="list-style-type: none"> - ASCE - AUS/NZ - EC3 - NAS Specification for cold-formed carbon steel which involves the four loading cases
Conclusions and remarkable observations	<ul style="list-style-type: none"> - ASCE specification, AUS/NZ standard, the EC3 and NAS specification are either unconservative or very conservative. - The studies carefully calibrate the coefficients of NAS specification for cold-formed austenitic and duplex stainless steel square and rectangular hollow sections.
Zhou & Young [21] University of Hong Kong (2007)	
Material	304 (high strength austenitic), Duplex (considered as a high strength steel)
Sections	SHS, RHS
Loading	IF, EF – Both of them seated on a fixed flat steel base plate (not considered in design rules)
Objective	- To compare 64 experimental results and 60 numerical

	simulations (using ABAQUS, S4R) against design rules. - To propose an unified equation which involves the four load status: IOF ETF, ITF
Specifications and methods involved	- American, Australian/New Zealand, European specifications - In addition, the test strengths were also compared with the nominal web crippling strengths predicted using the NAS Specification for cold-formed carbon steel which involves the four loading cases.
Conclusions and remarkable observations	- All specifications are very conservative excepting ITF load state for stainless steel type 304. - The results of NAS specification gives negative values because of the dimensions of the specimens are out of range. - An expression similar to NAS specification is proposed to predict the web crippling strength of cold-formed stainless steel hollow sections seated on a solid foundation and it is demonstrated that is safe and reliable.
Zhou & Young [22] University of Hong Kong (2007)	
Material	304 (high strength austenitic), Duplex (considered as a high strength steel)
Sections	2 SHS (50x50x1.5) and (150x150x6), 3 RHS (140x80x3), (160x80x3) and (200x110x4), 21 tests in total
Loading	IOF combining bending and web crippling
Objective	To compare 21 tests with design rules.
Specifications and methods involved	American, Australian/New Zealand
Conclusions and remarkable observations	- ASCE specification and AS/NZS are identical because AS/NZS standard has adopted the combined bending and web crippling design rules from the ASCE specification. - ASCE specification and AS/NZS standard conservatively predicted the strengths of cold-formed high strength stainless steel square and rectangular hollow sections subjected to combined bending and web crippling. - The bending and web crippling interaction equation of sections having single unreinforced webs in the ASCE specification and the AS/NZS standards is appropriate for cold-formed high strength stainless steel square and rectangular hollow sections

4 Design methods

This chapter introduces the basic principles of five design methods for cold-formed members. Cold-formed steel members are typically thin-walled, i.e., local **plate buckling** and **cross-section distortion** must be treated as an essential part of member design.

On the other hand, ferritic stainless steel is gaining increasing usage in the construction industry since these alloys generally have better engineering properties than austenitic grades, due to the lower chromium and nickel content (which also makes them less expensive).

Stainless steel alloys present a quite **nonlinear material** behavior with considerable strain hardening after the material is said to yield (both ferritic and austenitic). If this **strain hardening** is properly accounted for in cross-sectional and/or member design, the results might be less conservative and refined.

Most structural design codes define four classes of cross-section: class 1 (plastic), class 2 (compact), class 3 (semi-compact) and class 4 (slender). Class 1 and 2 are fully effective under pure compression and are capable of attaining their full plastic moment in bending (Class 2 cross-sections, however, have a lower deformation capacity). Class 3 cross-sections are fully effective in pure compression, but local buckling prevents attainment of the full plastic moment in bending; bending moment resistance is therefore limited to the elastic moment.

In Europe, cold-formed stainless steel members have been traditionally verified following an extension of the rules which apply to cold-formed sections with carbon steel. Contrarily to carbon steel though, such alloys do not present sharply defined elastic, perfectly-plastic material behavior. The principal concepts that underpin current metallic structural design codes were, however, developed on the basis of such bilinear material behavior.

Thus, a more sophisticated verification of stainless steel cold-formed sections could be erected by considering simultaneously features such as i) local plate buckling ii) distortional buckling iii) strain material hardening. The challenge of any cold-formed steel design method is to incorporate as many as these complex phenomena.

In the following, brief descriptions of the most outstanding design methods proposed in the literature are presented. Considerations of the aforementioned desirable features in cold-formed stainless steel design are highlighted for each method (as well as the lack of them). It is important to recognize in any discussion concerning these methods that none of them are fully theoretically correct. Rather, a complicated nonlinear problem is simplified in some manner so that engineers may have a working model to design from without resorting to testing or simulating every individual member.

4.1 The effective width method

The basis for the Effective Width Method is well explained and understood by most of researchers and engineers. The concept was first introduced by von Kármán [59]. It is based upon the replacement of the actual nonlinear distribution

of the stresses acting on the entire width of the plate by two equivalent uniform blocks distributed over two reduced effective width (see Fig. 1). Consistent refinements of the formulae have been proposed ever since the first publication and it is nowadays worldwide accepted for most designers as a relatively accurate, reliable method for calculation of thin-walled members. The method is also widely used in many industries for the design of ship and aerospace plated structures.

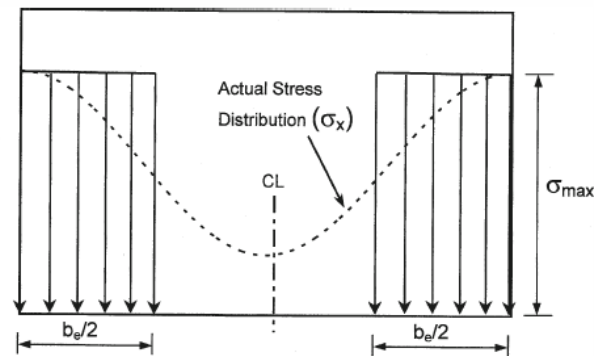


Figure 7. Typical effective width model of a compressed plate.

The magnitude of the uniform stress of each block is assumed to be equal to the actual stress at the edge of the plate. The two blocks (each of width $b_e/2$) are also assumed to have the same area as the actual stress distribution. By using this simplified concept, the maximum stress in the post-buckling state, is assumed to be carried entirely by both edges while the central region of the plate remains unstressed. Thus only a fraction of the width is considered in resisting the applied compression. When this stressed fraction of the plate attains levels of f_y over the whole length b_e , the load carrying capacity of the plate is exhausted. This approximation enables the designer to deal with a simplified stress distribution, rather than the highly non-linear one in post-buckling range. The method inherently assumes a sharply defined yield point in the material behaviour with no strain hardening after yielding.

The essential idea is that local plate buckling leads to reductions in the effectiveness of the plates that comprise a cross-section. In compressed class 4 plates belonging to a given cross-section, the key feature is to find an expression which links the reduction of the plate width with its non-dimensional slenderness. This relationship depends upon the actual stress distribution on the plate and on the boundary conditions (internal or outstand restrained elements). Once this reduction is obtained, the geometrical properties of the effective cross-section must be recalculated and thus, the novel stress distribution. For cold-formed arbitrary sections, this method might become highly iterative yet relatively simple.

The effective cross-section gives the following features:

- Provides a clear model for the locations in the cross-section where material is ineffective in carrying load.
- Leads to the notion of neutral axis shift in the section due to local buckling.
- Provides an obvious means.

4.2 The continuous strength method

The resistance of structural cross-sections is a continuous function of the slenderness of the constituent plate elements. The resistance based upon the assignment of cross-sections to discrete behavioural classes is a useful simplification of the factual behaviour of the plates. Dr. Gardner and his co-workers from the Imperial College of London have developed an alternative method for the verification of plated or cold-formed elements. In several research works, they demonstrate that the stepwise nature of the aforementioned classification of the cross-section does not reflect the observed physical response [60], [61]. As an alternative, they propose the continuous strength method, which employs i) more precise material modelling but also ii) does not discretize the behaviour of the cross-section in a stepwise fashion. The method is particularly suitable for stainless steel cross sections since it accounts for its deformation capacity and strain hardening (it is also suitable for other metallic materials with rounded stress-strain behaviour).

A key feature of such method is the cross-section deformation capacity, which has been derived from the end-shortening δ_u corresponding to the ultimate load F_u from stub columns tests. Subsequently, the average strain at ultimate load ε_{LB} is determined by dividing δ_u by the stub columns length L . Cross-section deformation capacity is therefore defined by the normalised strain load $\varepsilon_{LB}/\varepsilon_0$ (where $\varepsilon_0 = f_y/E$). Another key feature of the continuous strength method is the definition of a continuous non-dimensional numerical measure of the deformation capacity of the cross-section. This concept entirely replaces the cross-section classification. These magnitudes has been derived for cross-sections comprising flat plates and for circular hollow sections CHS. The adopted measures of slenderness λ_c (CHS) and λ_p (Plates) are given in eq. (2).

$$\bar{\lambda}_p = \frac{\sqrt{12 \cdot (1 - \nu^2) \cdot 235}}{\pi \cdot \sqrt{E \cdot k_\sigma}} \cdot \left(\frac{b}{t \cdot \varepsilon} \right) \quad \bar{\lambda}_c = \frac{235 \cdot \sqrt{3 \cdot (1 - \nu^2)}}{2 \cdot E} \cdot \left(\frac{D}{t \cdot \varepsilon^2} \right) \quad (2)$$

With both magnitudes defined, relationships between the deformation capacity and the non-dimensional slenderness are derived empirically (given in eq. (3)).

$$\frac{\varepsilon_{LB}}{\varepsilon_0} = \frac{1.05}{\bar{\lambda}_p^{3.15 - 0.95 \cdot \bar{\lambda}_p}} \quad \frac{\varepsilon_{LB}}{\varepsilon_0} = \frac{0.07}{\bar{\lambda}_c^{1.51 - 2.55 \cdot \bar{\lambda}_c}} \quad (3)$$

The deformation capacity (and thus, ε_{LB}) can be obtained from geometrical and material properties of the section via the non-dimensional slenderness. The stress-strain relationship of the material (either bilinear for carbon steel or highly nonlinear for other metallic alloys) allows inferring the maximum attainable stress σ_{LB} . Finally, the cross-section compression $N_{c,Rd}$ and bending $M_{c,Rd}$ resistances might be calculated for different geometries following eq. (5).

$$N_{c,Rd} = \sigma_{LB} \cdot A \quad (4)$$

$$M_{c,Rd} = \int \sigma \cdot y \cdot dA \quad (5)$$

4.3 The direct strength method

If the reduction of the plate width is the fundamental concept behind the effective width method, then accurate member stability is the fundamental idea behind the Direct Strength Method. The Direct Strength Method [62] is predicated upon the idea that if an engineer determines all the elastic instabilities for the gross section (local M_{cr1} , distortional M_{crd} and global M_{cre} buckling) and also determines the moment that causes the section to yield M_y , then the strength can be directly determined (eq. (6))

$$M_n = f(M_{cr1}, M_{crd}, M_{cre}, M_y) \quad (6)$$

The method is essentially an extension of the use of column curves for global buckling, but with application to local and distortional buckling instabilities and appropriate consideration of post-buckling reserve and interaction in the modes. This method has been pioneered by Dr. Schafer and his co-workers from John Hopkins University in the United States. It has been somewhat inspired by outstanding research performed by Dr. Hancock into distortional buckling of rack-post sections. The Direct Strength Method can be alternatively used in the calculation of cold-formed sections in the specifications from the United States, Australia and New Zealand. It has an empirical basis, which is proven straightforward and reliable enough compared to the effective width method.

The method is applicable to the following calculations:

- Column and beam design
- Flexural, torsional, or torsional-flexural buckling when applicable
- Local buckling
- Distortional buckling.

Empirically-based, the method consists of defining a non-dimensional slenderness, which is a function of the critical buckling moment (or force, for columns) and the yield moment. It is worth pointing out that the relevant buckling load should be obtained by numerical calculations.

$$\lambda = \sqrt{\frac{M_y}{M_{cr,i}}} \quad (7)$$

Once the non-dimensional slenderness is defined, explicit functions of λ , M_y and $M_{cr,i}$ are determined empirically for each particular case (local, distortional, flexural or other types of buckling). It is noted that for the same member, several calculations shall be performed.

Attempts for using the Direct Strength Method in stainless steel design are less frequent though. The empirical basis of the formulation avoids a direct transition from carbon to stainless steel without performing new regression analysis. Some attempts for obtaining equations for distortional-buckling related formulae for stainless steel cross-sections have been proposed by [63], [64].

4.4 The Generalised Beam Theory (GBT)

The Generalised Beam Theory seeks, at the same time, both to unify and to extend conventional theories for the analysis of prismatic thin-walled structural members. The analytical treatment of several modes of deformation is united within a consistent notation. This allows elegant and computationally economical solutions to a wide range of complex problems and provides a natural transition from beam theory to folded plate theory. The development of the theory has been pioneered by Professor Schardt from the University of Darmstadt in Germany. Subsequently, Dr. Davies at the University of Salford in the U.K as well as Dr. Camotim and his co-workers at the Lisbon Technical University have extended quite profusely the applications of the GBT in research concerning cold-formed sections.

The GBT describes the behaviour of prismatic structures by ordinary uncoupled differential equations, using deformation modes for bending, torsion, distortion and local phenomena (by accounting for the deviating forces). The usual form of the equation is then:

$$E \cdot {}^k C {}^k V'''' - G \cdot {}^k D {}^k V'' + {}^k B {}^k V + \sum_i \sum_j {}^{ijk} k ({}^i W {}^j V')' = {}^k q \quad (8)$$

In this equation, E is the Young Modulus, G , the shear modulus, ${}^k C$, ${}^k D$ and ${}^k B$ are cross-sectional properties. ${}^k V$ is the generalized unit deformation in mode k , ${}^k q$ is the load applicable to mode k . ${}^i W$ is the warping stress resultant in the i th mode whereas ${}^{ijk} k$ is a three-dimensional array of second order terms which accounts for all the interactions between membrane and bending strains in the plates. These terms are linked so that the differential equations and the individual modes are not independent.

The GBT is intended to analyse the behaviour of elastic isotropic prismatic thin-walled members with arbitrary cross-sections. Its application involves the performance of two main tasks, namely (i) a “cross section analysis”, which concerns the identification of the deformation modes and the evaluation of the associated modal mechanical properties, and (ii) a member (first order, buckling) analysis, in which the appropriate differential equilibrium equations must be solved.

One of the strengths of Generalised Beam Theory is that it is possible to consider the significance of individual buckling modes and interestingly, a selected combination of them which makes it immediately clear which modes are important in any analysis. The method is particularly useful for determining all relevant buckling modes of an arbitrary cross-section by solving an eigenvalue problem in eq. (8). It requires, however, numerical programming for solving the set of differential equation for all relevant modes. The method is less likely for design purposes but it might be very useful for research purposes. Currently, no code exists in the public domain for the application of GBT; however, Camotim and Silvestre [65][65, 66] have recently supplied code focusing on distortional buckling of C and Z sections common in cold-formed steel.

4.5 The Erosion of Critical Bifurcation Load method (ECBL)

The ECBL approach, proposed by Dr. Dubina and his co-workers at the University of Timisoara, Romania, is a semi-empirical method which uses the rigid-plastic theory in order to introduce the local failure mode of thin-walled sections into the global behaviour of the member characterized by an Ayrton-Perry equation [67]. The method therefore gives the possibility to couple the potential local modes cold-formed section might undergo with the elastic overall ones. According to the authors, the main drawback of the method is the difficulties to evaluate the “erosion” of the critical load into the interactive slenderness range. This evaluation is said to be feasible if relevant experimental and/or numerical values are used and treated empirically (thus, the method is deemed as being semi-empiric).

Assuming the two theoretical simple instability modes that couple in a thin-walled compression member are the Euler instability N_E and the local instability N_L , the maximum erosion of critical load, both due to the imperfection and interaction effects, occurs in the coupling point M (see Figure 8). The interactive buckling load $N(\lambda, N_L, e)$, pass through this point and the corresponding value of ultimate buckling load is:

$$N_N = (1-e) \cdot N_L \quad (9)$$

where e is the erosion factor

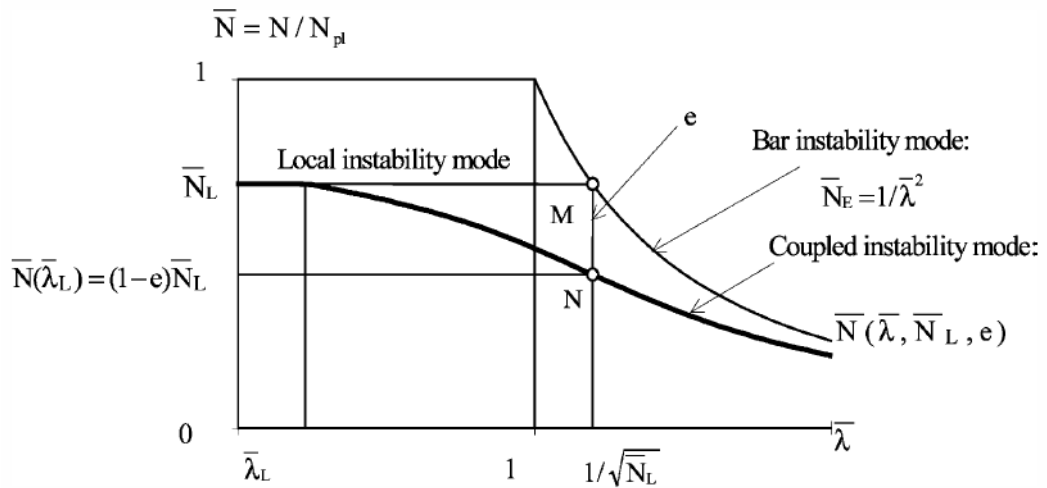


Figure 8.

There are two practical ways that can be used to evaluate the erosion factor:

- The experimental procedure which involves a statistical analysis of a representative series of test results corresponding to specified cross-section shapes, type of steel.
- The numerical nonlinear analysis of the behaviour of thin-walled columns in the vicinity of the critical bifurcation point.

The method might be considerably straightforward if consistent and appropriate expressions of the erosion factor are given for different types of materials and shapes of the cross-section. This feature would imply the need of a plethora of expressions for different structural alternatives.

5 Solution schemes in FE analysis

Typically, the peak and collapse load is investigated with non-linear Riks (arc-length) method that provides good results that are not very sensitive to the initial settings. According to the parametric study [68] the variation of peak loads is within 5%. The initial settings of Riks method include the length of initial step as well as artificial damping configuration if used.

Although the arc-length method is able to plot also descending part of the load-displacement relationship, it is usually preferred to stop the calculation when the peak load is reached. Limiting factor according to Eurocode 3, Part 1-5 [69] is also tensile strain of 5% which can be integrated into the material model.

5.1 Element selection

The typical model sensitivity for element and mesh selection is up to 15% of peak load [68]. The following options may be considered.

5.1.1 General purpose shell elements

FEM solvers offer usually several types of general purpose linear shell elements with finite strain formulation and 6 degrees of freedom at each node. Basic S4 (Abaqus) shell elements are usually strain-locking in out-of-plane bending situations and user needs at least 5 elements per face to avoid it [68]. On the other hand, S4R (Abaqus) elements do not have this problem, but may provide inaccurate results due to hourglassing that occurs in linear elements with reduced integration.

5.1.2 Thin shell elements

Thin shells can be modelled also with small strain elements, where the transverse shear deformation is neglected resulting in 5 degrees of freedom per node. Linear elements with 4 nodes (S4R5 in Abaqus) suffer the same problems as S4R and thus they are not suitable for the considered analysis. There are also two quadratic elements available in Abaqus: S8R5 and S9R5 with 8 nodes and 9 nodes respectively, where the hourglassing is not an issue due to their nonlinear nature. According to [70] “S8R5 may give inaccurate results for buckling problems of doubly curved shells due to the fact that the internally defined centre node may not be positioned on the actual shell surface. Element type S9R5 should be used instead.” It should be also noted that using thin shell elements without in-plane shear we can lose a small amount of buckling modes (identified as “other” in [71]) in which the Vlasov’s hypothesis is not valid.

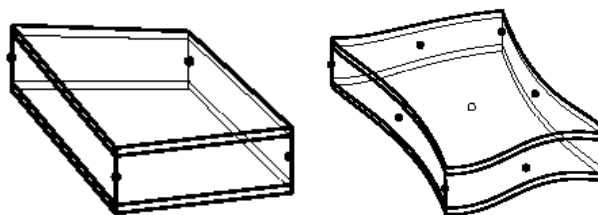


Figure 9. Typical linear and quadratic shell elements.

5.1.3 Shell elements in Abaqus

Linear S4R and quadratic S9R5 elements are widely employed in cold-formed steel numerical calculations. The former ones are used [29, 72] for their simple application and because they are also included in Abaqus/GUI interface, while the latter ones are preferred in recent studies [11, 73, 74] as slightly more accurate and much more robust. Quadratic elements also offer more flexibility when modelling rounded corners avoiding large aspect ratios.

5.1.4 Beam elements for the overall buckling behaviour

As an alternative to restrained shell models, also beam elements can be used for calculation of overall buckling of cold-formed stainless steel members [75]. In that case, a finite element solver is needed that is able to insert initial stress or strain pattern on a cross-section as well as enhanced material properties if needed. Abaqus allows modelling of the former by inserting initial stress or strain into the section points. Additionally in case of open cross section, the allowance of warping stresses and deformation is needed in element. For example, the linear 3D beam element (B31OS in Abaqus) is suitable for modelling of overall behaviour of members with open-section.

5.1.5 Mesh size

According to the parametric study [68], there should be more than 5 elements with linear shape function (S4R) per buckling half-wave in order to avoid locking. However, elements with quadratic shape function (S9R5) provide acceptable results starting with only one element per buckling half-wave.

5.2 Geometric imperfections

There are several ways of modelling geometric imperfections. In case of simulating the experiment (physical reality), usually the real initial imperfection data are inserted into a model either in form of the whole deformed geometry or as a real amplification of idealized imperfect shape. The models are preferably simulated several times with different imperfection distribution.

For the design (modelling) convenience of a cold-formed member, the idealized imperfection distribution is needed and it is usually obtained from linear elastic analysis (LEA) of the finite element model. In some cases, only the first elastic buckling mode is used, but it is recommended to perform linear combination of several representative modal shapes (global, distortional, local or another). Such modes are not always the ones with lowest critical loads, and the selection of proper shape can be difficult. The buckling mode decomposition was studied in [71] using a constrained Finite Strip Method (cFSM). The selected deformation is then amplified either to match initial geometric imperfections expected in the member or to accommodate also effects of residual stresses together with enhanced corner properties, material anisotropy and other model uncertainties. The higher critical modes amplitudes are usually reduced. According to Eurocode 3, Part 1-5 [69] “*the accompanying imperfections may have their values reduced to 70%*”.

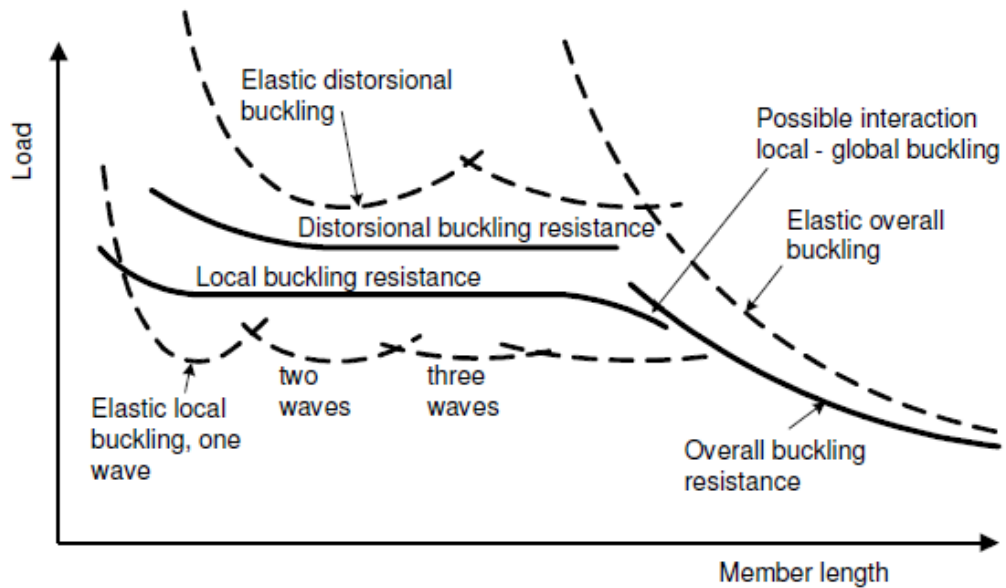


Figure 10. Elastic buckling resistance as a function of member length [1].

5.3 Local buckling

Local buckling can be identified as mode, where line junctions and angles between elements remain the same; however the cross-sectional shape changes within the element. Vlasov's hypothesis should be valid in those cases (no in-plane shear strain can be simulated by thin-shell elements).

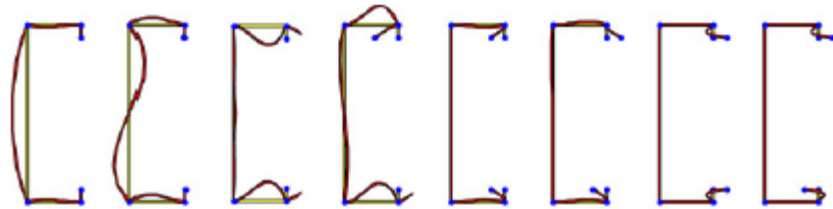


Figure 11. Local buckling modes [71].

Amplitude of local initial imperfection of plate $a \times b$ is smaller of values $a/200$ or $b/200$ according to Eurocode 3, Part 1-5 [69].

5.4 Distortional buckling

Distortional buckling is a mode that involves changes in cross-sectional shape excluding local buckling. Additionally to Vlasov's hypothesis, longitudinal warping is not constantly equal to zero, while the whole cross-section is in transverse equilibrium. The last requirement ensures that distortional buckling occurs only in open sections that are able to warp.

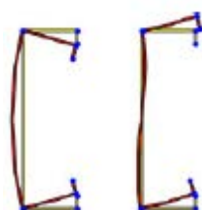


Figure 12. Distortional buckling modes [71].

5.5 Global (overall) buckling

In global buckling, the member bends and/or twists simultaneously without change of cross-sectional shape. This failure is observed in compressed and/or bended slender members; however, it was theoretically identified also with tensile loading. To separate the global buckling mode from the other eigenvalue solutions, several techniques have been adopted including cFSM [71]. While the cross-section remains undistorted, longitudinal warping has to be allowed and Vlasov's hypothesis should be valid (there is no in-plane or transverse shear strain and longitudinal deformation is linear within a flat part of cross-section). In FEM solvers, the constraint can be simulated by using thin shell elements without in-plane strain and connecting cross-sectional nodes together with membrane elements [76]. Another possibility is to use beam elements [75] where it would be, however, difficult to transform deformed shape directly to shell model.

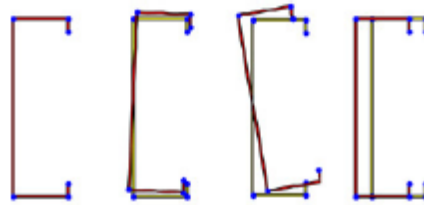


Figure 13. Global buckling modes [71].

The recommended amplitudes of equivalent global imperfections to match Eurocode 3, Part 1-1 [77] strength curves are given in the following table:

Table 6. Equivalent initial imperfections recommended by Eurocode 3, Part 1-1 [77].

Buckling curve	Elastic analysis	Plastic analysis	Imperfection factor
a_0	1/350	1/300	0.13
a	1/300	1/250	0.21
b	1/250	1/200	0.34
c	1/200	1/150	0.49
d	1/150	1/100	0.76

which originates from:

$$e_0 = \alpha \left(\bar{\lambda} - \bar{\lambda}_0 \right) \frac{W_{el}}{A} \text{ for elastic analysis and} \quad (10)$$

$$e_0 = \alpha \left(\bar{\lambda} - \bar{\lambda}_0 \right) \frac{W_{pl}}{A} \text{ for plastic analysis.} \quad (11)$$

Another possibility is to insert only geometric imperfections that are usually in range from $L/1000$ to $L/2000$ together with enhanced corner properties and residual stresses or strains. The geometric imperfection of $L/1000$ was used as a basis of Eurocode 3 buckling curves.

6 Material models

The increased amount of structural applications of metallic materials such as stainless steel and aluminum alloys brought up a question of proper implementation of their non-linear stress-strain behavior in the design process. Number of material models has been developed during the last decades mostly originating from Ramberg-Osgood law (Chapter 6.2) and some of them are already implemented in the European, Australian and American standards. All those models with different level of complexity and different limitations rely on set of prescribed material parameters usually obtained from material tests. Some of them are developed for special purposes showing good agreement with test results at very high strains while others are focused on the area of expected behavior of material embedded in the load bearing structure. Although elastic – perfectly plastic material was studied in connection with stainless-steel numerical modelling [63], it is not discussed in this document because it shows very poor match to the real material behaviour.

6.1 Holmquist & Nadai model (1939)

The need for more accurate mathematical description of stress-strain relationship of materials without sharp yield point appeared already in 1939, when Holmquist and Nadai [78] used the polynomial equation to describe the material behaviour beyond the proportional limit σ_p to predict the buckling resistance of metal (stainless steel, iron and brass) tubes.

$$\varepsilon = \begin{cases} \frac{\sigma}{E_0} & \text{for } \sigma \leq \sigma_p \\ \frac{\sigma}{E_0} + \varepsilon_y \left(\frac{\sigma - \sigma_p}{\sigma_y - \sigma_p} \right)^n & \text{for } \sigma > \sigma_p \end{cases} \quad (12)$$

6.2 Ramberg & Osgood model (1943)

The similar non-linear model [79] was developed for aluminium alloys but it is used nowadays also for stainless steel and other metallic materials.

$$\varepsilon = \frac{\sigma}{E_0} + K \left(\frac{\sigma}{E_0} \right)^n \quad (13)$$

where the stress-strain relationship can be exactly the same as in Holmquist and Nadai model assuming that the proportional limit is 0 and the Ramberg-Osgood constant K is:

$$K = \varepsilon_y \left(\frac{E_0}{\sigma_y} \right)^n \quad (14)$$

6.3 Hill's modification (1944)

During the next development of Ramberg-Osgood model for stainless steel the offset yield stress was agreed to be 0.2% proof stress [80].

$$\varepsilon = \frac{\sigma}{E_0} + 0.002 \left(\frac{\sigma}{\sigma_{0.2}} \right)^n \quad (15)$$

where the Ramberg-Osgood constant n is calculated from the proportional limit 0.01%.

$$n = \frac{\ln(20)}{\ln(\sigma_{0.2}/\sigma_{0.01})} \quad (16)$$

This model is included in AS/NZS 4373:2001 [35], Eurocode 3, Part 1-4 [33] and SEI/ASCE [34], where also secant or tangent modulus is required for the design purposes:

$$E_s = \frac{\sigma}{\varepsilon} = \frac{E_0}{1 + 0.002 E_0 \left(\sigma^{n-1} / \sigma_{0.2}^n \right)} \quad (17)$$

$$E_t = \frac{d\sigma}{d\varepsilon} = \frac{E_0 \sigma_{0.2}}{\sigma_{0.2} + 0.002 n E_0 \left(\sigma / \sigma_{0.2} \right)^{n-1}} \quad (18)$$

6.4 Mirambell & Real two-stage model (2000)

A new model developed from Ramberg-Osgood formulation [27] includes also strain hardening effect and is able to describe the material behaviour more precisely for strains larger than 0.2%. It introduces a new Ramberg & Osgood curve originating from 0.2% stress and continuing with the same tangent modulus but with different parameter of non-linearity (called “m” in this case).

$$\varepsilon = \begin{cases} \frac{\sigma}{E_0} + 0.002 \left(\frac{\sigma}{\sigma_{0.2}} \right)^n & \text{for } \sigma \leq \sigma_{0.2} \\ \frac{\sigma - \sigma_{0.2}}{E_{0.2}} + \varepsilon^* \left(\frac{\sigma - \sigma_{0.2}}{\sigma_u - \sigma_{0.2}} \right)^m + \varepsilon_{0.2} & \text{for } \sigma > \sigma_{0.2} \end{cases} \quad (19)$$

$$\text{where } \varepsilon^* = \varepsilon_u - \varepsilon_{0.2} - \frac{\sigma_u - \sigma_{0.2}}{E_{0.2}}$$

$$0.2\% \text{ strain is } \varepsilon_{0.2} = \frac{\sigma_{0.2}}{E_0} + 0.002 \quad (20)$$

$$\text{and the tangent modulus } E_{0.2} = \frac{E_0}{1 + 0.002 n (E_0 / \sigma_{0.2})}$$

6.5 Rasmussen's modification (2003)

The following study [81] extends Mirambell & Real model reducing its original six parameters to three.

$$\varepsilon = \begin{cases} \frac{\sigma}{E_0} + 0.002 \left(\frac{\sigma}{\sigma_{0.2}} \right)^n & \text{for } \sigma \leq \sigma_{0.2} \\ \frac{\sigma - \sigma_{0.2}}{E_{0.2}} + \varepsilon^* \left(\frac{\sigma - \sigma_{0.2}}{\sigma_u - \sigma_{0.2}} \right)^m + \varepsilon_{0.2} & \text{for } \sigma > \sigma_{0.2} \end{cases} \quad (21)$$

$$\text{where } \varepsilon^* = 1 - \frac{\sigma_{0.2}}{\sigma_u}, \quad m = 1 + 3.5 \frac{\sigma_{0.2}}{\sigma_u}$$

The model is based on assumption that plastic ultimate strain can be approximated with total ultimate strain with a very small error and it is a function of the 0.2% and ultimate stresses ratio. Also the second non-linear parameter “m” is expressed as the function of the same ratio and both equations originate from the experimental data collected by Rasmussen [81]. The third parameter reduced in Rasmussen's modification of Mirambell & Real model is the ultimate stress that can be calculated from the following relations:

$$\frac{\sigma_{0.2}}{\sigma_u} = \begin{cases} 0.2 + 185(\sigma_{0.2}/E_0) & \text{for austenitic and duplex alloys} \\ \frac{0.2 + 185(\sigma_{0.2}/E_0)}{1 - 0.0375(n-5)} & \text{for all alloys} \end{cases} \quad (22)$$

Rasmussen's model is included also in Annex C of Eurocode 3, Part 1-4 [33].

6.6 Gardner's modification (2006)

Gardner proposed another interesting modification of Mirambell & Real material model, where the second part of Ramberg-Osgood curve passes through 1.0% proof stress instead of ultimate stress [82]. This approach is said to be more convenient because it can include also compressive behaviour (with a good agreement up to 10% strain) where there is no ultimate value and finally, the 1.0% stress is closer to the mostly used area of application of the material model.

$$\varepsilon = \begin{cases} \frac{\sigma}{E_0} + 0.002 \left(\frac{\sigma}{\sigma_{0.2}} \right)^n & \text{for } \sigma \leq \sigma_{0.2} \\ \frac{\sigma - \sigma_{0.2}}{E_{0.2}} + \left[0.008 - (\sigma_{1.0} - \sigma_{0.2}) \left(\frac{1}{E_{0.2}} - \frac{1}{E_0} \right) \right] \left(\frac{\sigma - \sigma_{0.2}}{\sigma_{1.0} - \sigma_{0.2}} \right)^{n0.2-1.0} + \varepsilon_{0.2} & \text{for } \sigma > \sigma_{0.2} \end{cases} \quad (23)$$

Gardner's model also reduces number of necessary material parameters by suggesting a 1.0% and 0.2% proof stress ratio for different steel and aluminium grades and also because the difference between 1.0% and 0.2% plastic strain is already known.

6.7 Quach's three-stage model (2008)

Considering the increasing difference between true stress/strain and nominal stress/strain curve in higher strains, three-stage model was developed by Quach et al [83]. This model uses nominal-to-true values transformation for stresses and strains higher than 1.0% proof values. This model was developed especially for investigating of stresses created during the cold-forming process at high plastic strain rates. In mathematical terms, it is a hybrid of nominal (up to 1.0%) and true (over 1.0%) values.

$$\varepsilon = \begin{cases} \frac{\sigma}{E_0} + 0.002 \left(\frac{\sigma}{\sigma_{0.2}} \right)^n & \text{for } \sigma \leq \sigma_{0.2} \\ \frac{\sigma - \sigma_{0.2}}{E_{0.2}} + \left[0.008 - (\sigma_{1.0} - \sigma_{0.2}) \left(\frac{1}{E_{0.2}} - \frac{1}{E_0} \right) \right] \left(\frac{\sigma - \sigma_{0.2}}{\sigma_{1.0} - \sigma_{0.2}} \right)^{n_{0.2-1.0}} + \varepsilon_{0.2} & \text{for } \sigma_{0.2} < \sigma \leq \sigma_{1.0} \\ \frac{\sigma - a}{b \pm \sigma} & \text{for } \sigma_{1.0} < \sigma \end{cases} \quad (24)$$

where a and b are calculated to match true stress and strain. This can be useful for the direct implementation of model points into FEM solvers, however, it seems to be more convenient to perform transformation of all stages afterwards as it is discussed in later chapters.

6.8 The generalized multi-stage model (2010)

We propose to use Mirambell & Real approach to generalize the material model to simple multi-stage form that is able to intersect any number of points given (e.g. measured). The generalized mode described in this chapter unifies all of previous approaches in a single definition which enables easy and transparent cross-platform handling of the material model in a multi-disciplinary global environment. The model is in dependent on particular testing standards giving a great flexibility to designers and program developers. It is suitable for modern information exchange technologies such as CIS/2, BIM or IFC and standardized product models such as LPM/6. The inverse formulation of the material model is addressed in the study since the expression of stress being a function of strain can be preferred in some cases.

$$\varepsilon = \frac{\sigma - \sigma_i}{E_i} + \varepsilon_i^* \left(\frac{\sigma - \sigma_i}{\sigma_{i+1} - \sigma_i} \right)^{n_i} + \varepsilon_i^{pl} + \frac{\sigma_i}{E_0} \text{ for } \sigma_i < \sigma \leq \sigma_{i+1} \quad (25)$$

where the tangent modulus of the next segment is

$$E_{i+1} = \frac{E_i}{1 + \varepsilon_i^* n_i \frac{E_i}{\sigma_{i+1} - \sigma_i}} \quad \text{and} \quad \varepsilon_i^* = (\varepsilon_{i+1}^{pl} - \varepsilon_i^{pl}) - \left(\frac{\sigma_{i+1} - \sigma_i}{E_i} - \frac{\sigma_{i+1} - \sigma_i}{E_0} \right)$$

The non-linear parameter n_i can be calculated by measuring one additional point “ j ” between “ i ” and “ $i+1$ ”.

$$n_i = \frac{\ln \left[\frac{(\varepsilon_{i+1} - \varepsilon_i)}{(\varepsilon_j - \varepsilon_i)} \right]}{\ln \left[\frac{(\sigma_{i+1} - \sigma_i)}{(\sigma_j - \sigma_i)} \right]}$$

The advantage of this generalized model is that it covers all present models and standards including basic one-stage Ramberg & Osgood model (15), two-stage Mirambell & Real (19) with Rasmussen’s (20) or Gardner’s (22) modifications as well, and it is flexible to accommodate even more parameters if provided.

With increasing number of segments also number of required parameters increases significantly. Actually, it is needed $2N+1$ parameters (where N is the number of segments) and one additional parameter for each point with the unknown plastic strain. However, it is possible to apply similar reduction techniques to that described in Rasmussen study [81].

The multi-stage equation (24) can for example produce following three-stage material curve for 0.2%, 1.0% and ultimate stress and strain measured.

$$\varepsilon = \begin{cases} \frac{\sigma}{E_0} + 0.002 \left(\frac{\sigma}{\sigma_{0.2}} \right)^{n_0} & \text{for } \sigma \leq \sigma_{0.2} \\ \frac{\sigma - \sigma_{0.2}}{E_{0.2}} + \varepsilon_{0.2}^* \left(\frac{\sigma - \sigma_{0.2}}{\sigma_{1.0} - \sigma_{0.2}} \right)^{n_{0.2}} + 0.002 + \frac{\sigma_{0.2}}{E_0} & \text{for } \sigma_{0.2} < \sigma \leq \sigma_{1.0} \\ \frac{\sigma - \sigma_{1.0}}{E_{1.0}} + \varepsilon_{1.0}^* \left(\frac{\sigma - \sigma_{1.0}}{\sigma_u - \sigma_{1.0}} \right)^{n_{1.0}} + 0.01 + \frac{\sigma_{1.0}}{E_0} & \text{for } \sigma_{1.0} < \sigma \leq \sigma_u \end{cases}$$

where

$$E_{0.2} = \frac{E_0}{1 + 0.002 n_0 \frac{E_0}{\sigma_{0.2}}}, \quad E_{1.0} = \frac{E_{0.2}}{1 + \varepsilon_{0.2}^* n_{0.2} \frac{E_{0.2}}{\sigma_{1.0} - \sigma_{0.2}}}$$

$$\varepsilon_{0.2}^* = 0.008 - \left(\frac{\sigma_{1.0} - \sigma_{0.2}}{E_{0.2}} - \frac{\sigma_{1.0} - \sigma_{0.2}}{E_0} \right)$$

$$\varepsilon_{1.0}^* = (\varepsilon_u^{pl} - 0.01) - \left(\frac{\sigma_u - \sigma_{1.0}}{E_{1.0}} - \frac{\sigma_u - \sigma_{1.0}}{E_0} \right)$$

(26)

The most simple way how to benefit from the proposed model in combination with Eurocode 3, Part 1-4 rules [33] is to use existing two-stage calculation in Annex C “Modelling of material behaviour” based on Rasmussen’s study where only the second non-linear parameter “ m ” can be more precisely calculated from 1,0% proof stress as demonstrated in Eq. (27) of this document. This agrees with Gardner’s recommendation of using 1.0% stress [82] and removes the uncertainty of the “ m ” parameter calculation originating from the limited collection of stainless steel material tests (including ferritic, austenitic and duplex grades) [81]. Unfortunately, the 1.0% values are requested only for austenitic steels according to EN 10088-2 [84] §7.3.4.

6.9 Models comparison

Selected models (Ramberg & Osgood – RO, Mirambell & Real – MR, Rasmussen – R, Gardner – G and Multi-Stage Eq.(26) - MS) are compared for the basic ferritic stainless steel grade 3Cr12 (grade 1.4003) with the following parameters:

Table 7 Comparison of different material models

Model parameters		Material model				
		RO	MR	R	G	MS
Initial Young’s modulus	E_0 [GPa]	220 ¹⁾	220 ¹⁾	220 ¹⁾	220 ¹⁾	220 ¹⁾
0,2% proof stress	$\sigma_{0.2}$ [MPa]	280 ¹⁾	280 ¹⁾	280 ¹⁾	280 ¹⁾	280 ¹⁾
1,0% proof stress	$\sigma_{1.0}$ [MPa]	-	-	-	319 ³⁾	319 ³⁾
Ultimate stress	σ_u [MPa]	-	450 ¹⁾	445 ²⁾	-	450 ¹⁾
Ultimate strain	ε_u [%]	-	40	37.1 ²⁾	-	40
0.0% to 0.2% non-linearity	n	7.0 ¹⁾	7.0 ¹⁾	12.2 ²⁾	7.4 ³⁾	7.0 ¹⁾
0.2% to 1.0% non-linearity	$n_{0.2-1.0}$	-	-	-	3.4 ³⁾	3.4 ³⁾
0.2% to ult. non-linearity	m	-	2.64 ⁴⁾	3.2 ²⁾	-	-
1.0% to ult. non-linearity	$n_{1.0-ult}$	-	-	-	-	2.0
¹⁾ Eurocode 3, Part 1-4 [33] ²⁾ Parameters calculated by Rasmussen’s model based on approximation of all available stainless steel data [81], value n recommended by Rasmussen ³⁾ Gardner’s recommended values for 3Cr12 grade stainless steel [82] ⁴⁾ Calculation based on Gardner’s recommended 1.0% proof stress						

Non-linear parameter m is calculated either by Rasmussen equation (21) based on test results statistics or (in the Mirambell-Real model) it was used 1.0% stress $\sigma_{1.0}$ proposed by Gardner to calculate this parameter:

$$m = \frac{\ln[(\varepsilon_u - \varepsilon_{0.2})/(\varepsilon_{1.0} - \varepsilon_{0.2})]}{\ln[(\sigma_u - \sigma_{0.2})/(\sigma_{1.0} - \sigma_{0.2})]} = 2.64 \quad (27)$$

Several assumptions had to be made to enable the construction of all models (e.g. ultimate strain and non-linear parameter $n_{1.0-ult}$ in multi-stage model).

It should be noted that Mirambell & Real and Rasmussen's models are almost identical; the only difference comes from different recommended non-linear parameters "n" for 3Cr12 steel and from simplification of 0.2% plastic strain in Rasmussen's model.

The Figure 14 and Figure 15 show that two-stage model (Mirambell & Real) can give results very close to the more complex three-stage model if its non-linear "m" parameter is calculated from the real stress/strain measurements (e.g. 1.0% stress given by Gardner). It is also demonstrated that Gardner's modification is more accurate up to 5% strain than Rasmussen's model (Figure 14) but it starts to differ from other models at higher strain ratios (Figure 15).

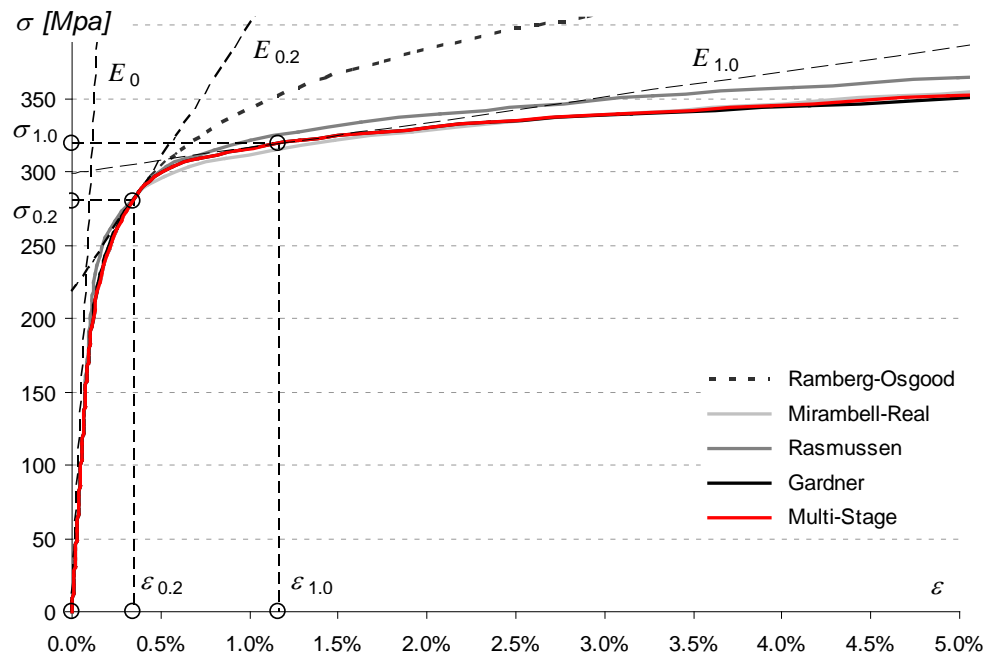


Figure 14. Comparison of different models of 3Cr12 steel up to 5% strain.

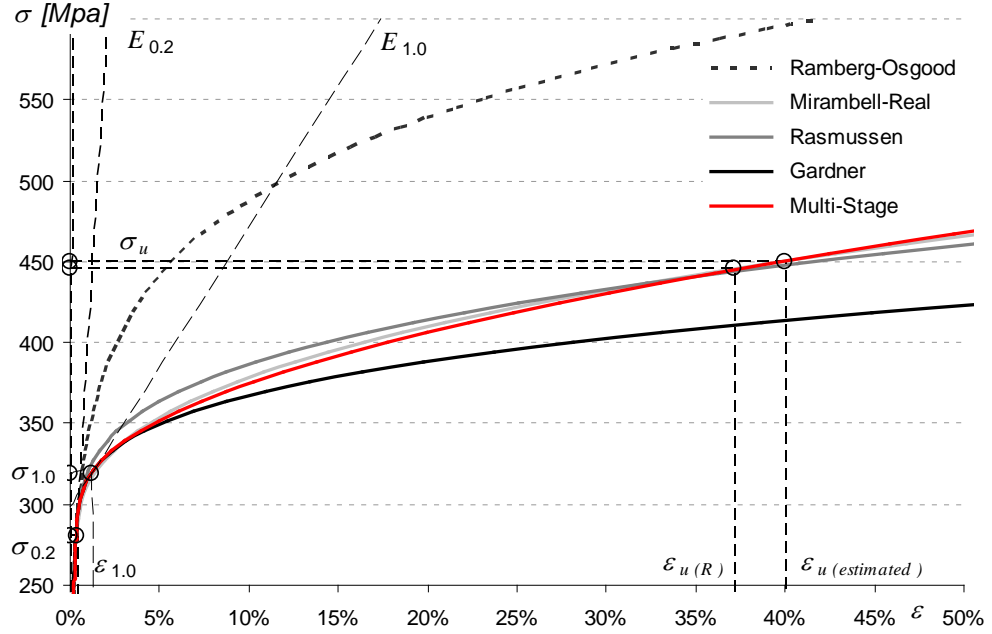


Figure 15. Comparison of different models of 3Cr12 steel up to 50% strain.

6.10 Explicit formulation of Ramberg-Osgood based models (2007–2009)

A study by Abdella [85] was published plotting approximated material curve of two-stage model, where stress is explicitly defined as function of strain following the power law with exponent “ p ”:

$$\sigma = \begin{cases} \frac{r\sigma_{0.2} \varepsilon / \varepsilon_{0.2}}{1 + (r-1)(\varepsilon / \varepsilon_{0.2})^p} & \text{for } \varepsilon \leq \varepsilon_{0.2} \\ \sigma_{0.2} + \frac{r_2\sigma_{0.2}(\varepsilon / \varepsilon_{0.2} - 1)}{1 + (r^* - 1)\left(\frac{\varepsilon / \varepsilon_{0.2} - 1}{\varepsilon_u / \varepsilon_{0.2} - 1}\right)^{p^*}} & \text{for } \varepsilon > \varepsilon_{0.2} \end{cases}, \text{ where}$$

$$p = r \frac{1-r_2}{r-1}, \quad p^* = r^* \frac{1-r_u}{r^*-1} \quad (28)$$

$$r = E_0 \frac{\varepsilon_{0.2}}{\sigma_{0.2}}, \quad r_2 = E_{0.2} \frac{\varepsilon_{0.2}}{\sigma_{0.2}}, \quad r^* = E_{0.2} \frac{\varepsilon_u - \varepsilon_{0.2}}{\sigma_u - \sigma_{0.2}}, \quad r_u = E_u \frac{\varepsilon_u - \varepsilon_{0.2}}{\sigma_u - \sigma_{0.2}}$$

$$E_u = \frac{E_{0.2}}{1 + (r^* - 1)m}$$

with a modification to match Gardner’s model [86]:

$$\sigma = \begin{cases} \frac{r\sigma_{0.2} \varepsilon/\varepsilon_{0.2}}{1+(r-1)(\varepsilon/\varepsilon_{0.2})^p} \text{ for } \varepsilon \leq \varepsilon_{0.2} \\ \sigma_{0.2} + \frac{r_2\sigma_{0.2}(\varepsilon/\varepsilon_{0.2}-1)}{1+(s-1)\left(\frac{\varepsilon/\varepsilon_{0.2}-1}{\varepsilon_{1.0}/\varepsilon_{0.2}-1}\right)^{p_1}} \text{ for } \varepsilon > \varepsilon_{0.2} \end{cases} \quad (29)$$

$$p = r \frac{1-r_2}{r-1}, \quad p_1 = s \frac{1-s_1}{s-1}$$

$$r = E_0 \frac{\varepsilon_{0.2}}{\sigma_{0.2}}, \quad r_2 = E_{0.2} \frac{\varepsilon_{0.2}}{\sigma_{0.2}}, \quad s = E_{0.2} \frac{\varepsilon_{1.0} - \varepsilon_{0.2}}{\sigma_{1.0} - \sigma_{0.2}}, \quad s_1 = E_{1.0} \frac{\varepsilon_{1.0} - \varepsilon_{0.2}}{\sigma_{1.0} - \sigma_{0.2}}$$

$$E_{0.1} = \frac{E_{0.2}}{1+(s-1)n_{0.2-1.0}}$$

6.11 Generalized explicit formulation of multi-stage model (2010)

Applying Abdella's approach (27) to the multi-stage model, inverse formulation yields to

$$\sigma = \sigma_i + \frac{E_i(\varepsilon - \varepsilon_i)}{1+(r_i-1)\left(\frac{\varepsilon - \varepsilon_i}{\varepsilon_{i+1} - \varepsilon_i}\right)^{p_i}} \text{ for } \varepsilon_i < \varepsilon \leq \varepsilon_{i+1}, \text{ where}$$

$$p_i = r_i \frac{1-s_i}{r_i-1}, \quad r_i = E_i \frac{\varepsilon_{i+1} - \varepsilon_i}{\sigma_{i+1} - \sigma_i}, \quad s_i = E_{i+1} \frac{\varepsilon_{i+1} - \varepsilon_i}{\sigma_{i+1} - \sigma_i} \quad (30)$$

$$E_{i+1} = \frac{E_i}{1+(r_i-1)n_i}$$

The explicit multi-stage model can for example produce following material curve for 0.2%, 1.0% and ultimate stress and strain measured (explicit formulation of Eq. (25)).

$$\sigma = \begin{cases} \frac{E_0\varepsilon}{1+(r_0-1)(\varepsilon/\varepsilon_{0.2})^{p_0}} \text{ for } \varepsilon \leq \varepsilon_{0.2} \\ \sigma_{0.2} + \frac{E_{0.2}(\varepsilon - \varepsilon_{0.2})}{1+(r_{0.2}-1)\left(\frac{\varepsilon - \varepsilon_{0.2}}{\varepsilon_{1.0} - \varepsilon_{0.2}}\right)^{p_{0.2}}} \text{ for } \varepsilon_{0.2} < \varepsilon \leq \varepsilon_{1.0} \\ \sigma_{1.0} + \frac{E_{1.0}(\varepsilon - \varepsilon_{1.0})}{1+(r_{1.0}-1)\left(\frac{\varepsilon - \varepsilon_{1.0}}{\varepsilon_u - \varepsilon_{0.2}}\right)^{p_{1.0}}} \text{ for } \varepsilon_{0.2} < \varepsilon \leq \varepsilon_{1.0} \end{cases}, \text{ where} \quad (31)$$

$$p_0 = r_0 \frac{1-s_0}{r_0-1}, \quad r_0 = E_0 \frac{\varepsilon_{0.2}}{\sigma_{0.2}}, \quad s_0 = E_{0.2} \frac{\varepsilon_{0.2}}{\sigma_{0.2}}$$

$$p_{0.2} = r_{0.2} \frac{1-s_{0.2}}{r_{0.2}-1}, \quad r_{0.2} = E_{0.2} \frac{\varepsilon_{1.0}-\varepsilon_{0.2}}{\sigma_{1.0}-\sigma_{0.2}}, \quad s_{0.2} = E_{1.0} \frac{\varepsilon_{1.0}-\varepsilon_{0.2}}{\sigma_{1.0}-\sigma_{0.2}}$$

$$p_{1.0} = r_{1.0} \frac{1-s_{1.0}}{r_{1.0}-1}, \quad r_{1.0} = E_{1.0} \frac{\varepsilon_u-\varepsilon_{1.0}}{\sigma_u-\sigma_{1.0}}, \quad s_{1.0} = E_u \frac{\varepsilon_u-\varepsilon_{1.0}}{\sigma_u-\sigma_{1.0}}$$

and tangent modulus can be calculated at each point using non-linear parameter “ n ”:

$$E_{0.2} = \frac{E_0}{1+(r_0-1)n_{0-0.2}}, \quad E_{1.0} = \frac{E_{0.2}}{1+(r_{0.2}-1)n_{0.2-1.0}}, \quad E_u = \frac{E_{1.0}}{1+(r_{1.0}-1)n_{1.0-u}}$$

6.12 Transformation for Abaqus solver

According to the Abaqus documentation [70], nominal (engineering) stress should be recalculated to true stress, and nominal (engineering) strain to logarithmic (true) strain using following equations:

$$\sigma_{true} = \sigma_{nom} (1 + \varepsilon_{nom}) \quad (32)$$

$$\varepsilon_{true} = \ln(1 + \varepsilon_{nom}) - \frac{\sigma_{true}}{E} \quad (33)$$

It should be noted that the calculation of true plastic strain can produce small negative values in the first few steps because it is not using transformed elastic modulus. However, the search for more appropriate solution is very complex topic that may involve also the thorough review of Abaqus internal calculation mechanism and the small negative values in our modelling can be neglected.

6.13 Overview of recommended material properties and designation

The most common stainless steel grades material properties are summarized in Table 8 recommended in European, Australian and American standards. The table includes material properties of those grades measured and collected by Rasmussen [81], Gardner [82], Rossi [87, 88] and Korvink [18]. The values of material properties can range between two numbers due to stainless steel anisotropy in the Table 8.

Unified Numbering System for Metals and Alloys (UNS) recognizes all stainless steels, including precipitation hardening stainless steel and iron-based superalloys with letter “S” followed by five digits (e.g. S30400). The corresponding designation according to BS, EN and ASCE is used in the Table 8.

Table 8. Overview of material properties for selected stainless steel grades.

			Austenitic		Ferritic			Duplex
Grade			304 (1/16 Hard in SEI/ASCE)	316 (1/16 Hard in SEI/ASCE)	409	3Cr12	430	2205
UNS BS EN Name			S30400 304S31 1.4301 X5CrNi18-10	S31600 316S31 1.4401	S40900 409S19 1.4512 X6CrTi12	S40977 - 1.4003 X2CrNi12	S43000 430S17 1.4016 X8Cr17	S31803/S32205 318S13 1.4462 X2CrNiMoN22-5-3
AS/NZS	E_0	GPa	195	195	185–200	195–230	185–200	195–205
	n	-	4.0–7.5	4.0–7.5	9.5–16	7.5–11.5	6.5–15	5.0–5.5
	$\sigma_{0.01}$	MPa	90–140	90–140	150–200	170–220	170–255	245–265
	$\sigma_{0.2}$	MPa	195–205	195–205	205–240	260–320	275–310	430–450
	σ_u	MPa	520	485	380	435–460	450	590–620
SEI/ASCE	E_0	GPa	193.1	193.1	186.2–200	-	186.2–200	-
	n	-	4.1–8.31	4.1–8.31	9.7–15.76	-	6.25–14.3	-
	$\sigma_{0.2}$	MPa	248.2–275.8	248.2–275.8	206.9–241.3	-	206.9–241.3	-
	σ_u	MPa	551.6–620.6	586.1–620.6	379.2	-	448.2	-
EC3-1.4	E_0	GPa	200	200	220	220	220	200
	n	-	6.0–8.0	7.0–9.0	9.0–16	7.0–11	6.0–14	5
	$\sigma_{0.2}$	MPa	190–230	200–240	210	260–280	240–260	450–480
	σ_u	MPa	500–540	500–530	380	450	400–450	640–660
Rasmussen	E_0	GPa	182–190	190	-	195	200	190–215
	n	-	4.49–7.87	5.88	-	12.2	6.37	4.85–10.6
	ε_u	-	0.34–0.65	0.51	-	0.38	0.48	0.22–0.32
	$\sigma_{0.01}$	MPa	178–297	190	-	215	200	310–526
	$\sigma_{0.2}$	MPa	297–612	316	-	275	320	575–699
	σ_u	MPa	611–780	616	-	444	622	805–878
Gardner	n	-	4.3–5.3	-	-	7.4	6.5	5
	$\sigma_{0.2}/\sigma_{0.01}$		1.20–1.25	-	-	1.14	1.16	1.15
Rossi	E_0	GPa	-	-	-	179–183	-	-
	n	-	-	-	-	11.4–15.1	-	-
	ε_u	-	-	-	-	0.266–0.313	-	-
	$\sigma_{0.01}$	MPa	-	-	-	247–281	-	-
	$\sigma_{0.2}$	MPa	-	-	-	315–347	-	-
	σ_u	MPa	-	-	-	608–637	-	-
Korvink	E_0	GPa	175–192	-	-	188–224	186–215	-
	ε_u	-	59.9–61.0	-	-	-	30.1–32.1	-
	$\sigma_{0.01}$	MPa	151–197	-	-	199–235	204–273	-
	$\sigma_{0.2}$	MPa	264–280	-	-	269–302	308–344	-
	σ_u	MPa	688–713	-	-	-	471–491	-

6.14 Material models for FE applications

For the application in SAFSS project it is recommended to use at least two-stage variant of generalized non-linear model. Good results can be achieved e.g. with

Rasmussen's modification of Mirambell & Real model, where parameter “ m ” is not calculated according to Rasmussen [81], but derived from 1.0% proof stress recommended by Gardner [82] as was demonstrated in previous example in MR curve Eq. (26).

In such model, the required set of parameters would be: the initial elastic modulus (E_0), stress levels at 0.01% strain ($\sigma_{0.01}$), 0.2% strain ($\sigma_{0.2}$), 1.0 % strain ($\sigma_{1.0}$), at the ultimate strain (σ_u) and the ultimate strain (ε_u).

Using these parameters, we can define the model input vectors for Eq. (24):

$$\begin{aligned} \sigma_i &\in \{0; \sigma_{0.2}; \sigma_u\} \\ \varepsilon_i^{pl} &\in \{0; 0.002; \varepsilon_u - \sigma_u/E_0\} \\ n_i &\in \left\{ \frac{\ln(20)}{\ln(\sigma_{0.2}/\sigma_{0.1})}; \frac{\ln[(\varepsilon_u - \sigma_u/E_0 - 0.002)/0.008]}{\ln[(\sigma_u - \sigma_{0.2})/(\sigma_{1.0} - \sigma_{0.2})]} \right\} \end{aligned} \quad (34)$$

The stress-strain relationship will be the same as in Mirambell & Real model (Eq. (19)).

7 Enhanced strength of material

7.1 Enhanced corner properties

Based on tensile test data, Karren proposed calculation model of enhanced corner strength based on r_i/t ratio [89]. Karren's model covers three fabrication processes (roll-forming, air-press braking and coin-press braking) and gives the increase of corner's yield strength as follows:

$$\Delta F_{y,c} = 0.6 \left[\frac{B_c}{(r_i/t)^m} - 1.0 \right] F_y, \text{ where} \quad (35)$$

$$B_c = 3.69 \left(\frac{F_u}{F_y} \right) - 0.819 \left(\frac{F_u}{F_y} \right)^2 - 1.79 \text{ and } m = 0.192 \left(\frac{F_u}{F_y} \right) - 0.068$$

The power model was later modified by van der Berg and van der Merwe in 1992 based on South African investigations of ferritic stainless steels. Nowadays it is included in AS/NZS 4673:2001 [35] in the following form:

$$\sigma_{02,c} = \frac{B_c \sigma_{02,v}}{(r_i/t)^m}, \text{ where} \quad (36)$$

$$B_c = 1.486 \left(\frac{f_{u,v}}{f_{y,v}} \right) - 0.21 \left(\frac{f_{u,v}}{f_{y,v}} \right)^2 - 0.128 \text{ and } m = 0.123 \left(\frac{f_{u,v}}{f_{y,v}} \right) - 0.068$$

The following two models proposed by Ashraf et al. in 2005 [90] are based on experimental data of cold-formed sections and few tubes:

$$\sigma_{02,c} = \frac{C_1 \sigma_{u,v}}{(r_i/t)^{C_2}}, \text{ where} \quad (37)$$

$$C_1 = -0.382 \left(\frac{\sigma_{u,v}}{\sigma_{02,v}} \right) + 1.711 \text{ and } C_2 = 0.176 \left(\frac{\sigma_{u,v}}{\sigma_{02,v}} \right) - 0.1496$$

The second one:

$$\sigma_{02,c} = \frac{1.881 \sigma_{02,v}}{(r_i/t)^{0.194}} \quad (38)$$

$$\sigma_{10,c} = 1.21 \sigma_{02,c} \quad (39)$$

$$\sigma_{u,c} = 0.75 \sigma_{02,c} \left(\frac{\sigma_{u,v}}{\sigma_{02,v}} \right) \quad (40)$$

Later, the model was modified by Cruise et al. and calibrated against experimental data to match roll-formed and press braked corner properties more precisely [91]:

$$\sigma_{02,pb,c} = \frac{1.673 \sigma_{0.2}}{\left(\frac{r_i}{t}\right)^{0.126}} \text{ for press-braked corners} \quad (41)$$

$$\sigma_{02,cr,c} = 0.83 \sigma_u \text{ for roll-formed corners} \quad (42)$$

A theoretical model was proposed by Rossi [92] calculating the enhanced strength from the explicit Ramberg-Osgood curve (Eq. (27))

$$\sigma_{02,c} = \sigma_{02,mill} + \frac{\sigma_{ult,mill}}{C_1 \left(\frac{r_i}{t/2}\right) + C_2 \left(\frac{r_i}{t/2}\right)^\alpha}, \text{ where} \quad (43)$$

$$C_1 = \frac{\varepsilon_{02}}{r_2} \frac{\sigma_{ult}}{\sigma_{02,mill}}, \quad C_2 = \frac{(r^* - 1) \varepsilon_{02}}{r_2 (\varepsilon_u - \varepsilon_{02})^{p^*}} \frac{\sigma_{ult}}{\sigma_{02,mill}} \text{ and } \alpha = 1 - p^*$$

Parameters r_2 , r^* and p^* are calculated according to Eq. (27).

7.2 Corner extensions

Based on experiments from carbon steel, Karren proposed to extend enhanced corner properties by distance equal to t in flat parts of section [89]. However, it was found that the extension should be even longer in stainless steels. Abdel-Rahman proposed different approach [93] for cold-formed carbon steel lipped sections, where the distance is $0.5\pi r_i$. According to Gardner's study in 2002 the distance should be $2t$. Finally, Cruise et. al [91] proposed together with different enhanced corner properties calculation a different approach to corner extensions for roll-formed and press-braked steel (Figure 16).

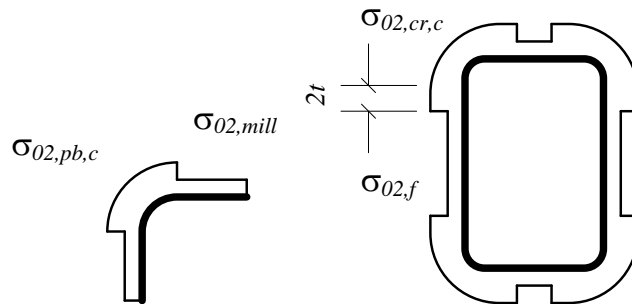


Figure 16. Enhanced corner properties distribution according to Cruise et al. [91] for press-braked sections (left) and cold-rolled sections (right).

7.3 Enhanced cold-rolled faces properties

For design models using test-data obtained from flat products, it is needed to enhance also flat segment's material properties due to cold-working. One possibility is to use following calculation published by Cruise et al. [91]:

$$\sigma_{02,f} = \frac{0.85 \sigma_{02,mill}}{-0.19 + \frac{1}{12.42 \left[\pi t / 2 (b+d) \right] + 0.83}} \quad (44)$$

$$\sigma_{ult,f} = \sigma_{ult,mill} \left[0.19 \left(\frac{\sigma_{02,f}}{\sigma_{02,mill}} \right) + 0.85 \right]$$

Another model proposed by Rossi [92] uses the same calculation as enhanced strength in corners (Eq. (42)), only the corner radius r_i is replaced by $(b+d)/\pi$, where b and d are rectangular hollow section width and height.

$$\sigma_{02,f} = \sigma_{02,mill} + \frac{\sigma_{ult,mill}}{C_1 \left[\frac{(b+d)/\pi}{t/2} \right] + C_2 \left[\frac{(b+d)/\pi}{t/2} \right]^\alpha}, \text{ where} \quad (45)$$

$$C_1 = \frac{\varepsilon_{02}}{r_2} \frac{\sigma_{ult}}{\sigma_{02,mill}}, \quad C_2 = \frac{(r^*-1)\varepsilon_{02}}{r_2(\varepsilon_u - \varepsilon_{02})^{p^*}} \frac{\sigma_{ult}}{\sigma_{02,mill}} \text{ and } \alpha = 1 - p^*$$

Parameters r_2 , r^* and p^* are calculated according to Eq. (27).

7.4 Average yield strength

In order to obtain data compatible with Eurocode calculations (e.g. cross sectional resistance and buckling resistance in axially loaded members with a fully effective cross-section), average yield strength value is needed for cold-formed members. Eurocode 3, Part 1-3 [1] proposes following equation:

$$f_{ya} = f_{yb} + (f_u - f_{yb}) \frac{knt^2}{A_g}, \text{ where } f_{ya} \leq \frac{f_u + f_{yb}}{2} \quad (46)$$

f_{yb} is the basic yield strength, A_g is the gross cross-sectional area, $k = 7$ for roll-forming and $k = 5$ otherwise, n is the number of 90° bends. However, this equation is not valid in the present version of supplementary rules for stainless steel [33] and the only way to get an average yield strength is to perform full-size member tests.

8 Residual stresses

According to Gardner's study, residual stresses from welding of cold-formed hollow sections can be neglected; however, residual stresses from bending should be accounted for in the numerical analysis [94]. There are several ways of implementation of this effect. Using Eurocode's equivalent imperfections together with the proper buckling curve is one possibility although it is quite rough approach. In many studies the problem with inserting residual stress pattern was avoided by material model derived from tests on straightened coupons cut from cold-formed sections. The most accurate way, however, is using initial conditions in FE solver and define stress pattern over the cross-section.

8.1 Bending residual stresses

Bending residual stresses are typical for cold-formed members with tensile extreme values on the outer surface and compressive values on the inner surface of curvature. They are usually combined with the membrane component which is very small compared to the bending part and is often neglected. In real members the stress distribution is non-linear, however, it is sufficient to assume the linear distribution in most cases [95]. As a result of coiling, uncoiling and levelling of annealed material, residual stresses greater than the original yield strength may appear together with the enhanced material strength. Their magnitude is dependent on the curvature of the coil.

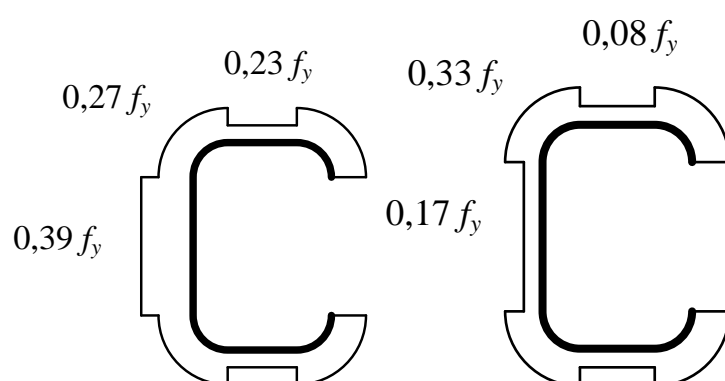


Figure 17. Residual stresses in cold-rolled (left) and press-braked sections (right) according to Schafer and Peköz [68].

The typical forming process of rectangular hollow sections include forming of a tube followed by seam welding and consequent forming of a rectangular shape. Larger hollow sections can be welded from two channels on the opposite sides. Residual stresses originating from those steps are mainly bending stresses, however, it is important to distinguish between the cold-rolling and press-braking process typical for the open sections. The model of residual stress distribution in carbon steel sections was proposed by Schafer [68] (Figure 17) and later revised by Gardner and Cruise [94] for stainless steel members (Figure 18).

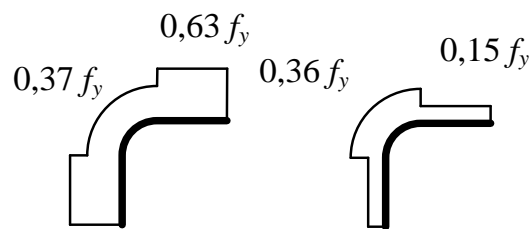


Figure 18. Residual stresses in cold-rolled (left) and press-braked sections (right) according to Gardner and Cruise [94].

8.2 Axial (membrane) residual stresses

For hot-rolled and welded sections axial (membrane) stresses are usually very significant. Hot-rolled stainless steel sections are fairly uncommon; however, they have been introduced in several studies. Axial residual stresses in hot-rolled sections are mainly caused by differential cooling of material with variable thickness. Their variation is usually low compared to the welded sections.

9 Strength curves

The first serious attempts to describe the real global behaviour of compressed members started almost two hundred years after Euler's theory of elastic stability [96] was published, according which the reduction factor could be described as a function of non-dimensional slenderness (46).

$$\chi = \frac{1}{\bar{\lambda}^2}, \text{ where } \bar{\lambda} = \sqrt{\frac{Af_y}{N_{cr}}} = \frac{L_{cr}/i}{\pi} \sqrt{\frac{f_y}{E}} \quad (47)$$

Nowadays the reduction proposed by most design codes already includes the effect of initial geometric and material imperfections or gradual yielding of material.

9.1 Ayrton-Perry curve (1886)

The calculation in Eurocode is based on Ayrton-Perry formula of initially imperfect compressed member. The basic form of Ayrton-Perry buckling curve is:

$$(\sigma_{cr} - \sigma_b)(f_y - \sigma_b) = \sigma_b \sigma_{cr} \eta \quad (48)$$

where $\sigma_{cr} = N_{cr}/A$ is critical buckling stress, $\sigma_b = N/A$ is compressive stress and $\eta = e_0 A/W$ is imperfection factor. The imperfection factor can be also written using slenderness ratio $\lambda = L/i$:

$$\eta = \frac{e_0 \lambda}{L(i/v)} \quad (49)$$

where v is the distance from neutral axis to extreme fibres. Introducing slenderness plateau we can write:

$$\eta = \frac{e_0 \pi \sqrt{E/f_y}}{L(i/v)} (\bar{\lambda} - \bar{\lambda}_0) = \frac{\lambda_1}{\gamma(i/v)} (\bar{\lambda} - \bar{\lambda}_0), \text{ where } \gamma = L/e_0 \text{ and } \lambda_1 = \pi \sqrt{E/f_y} \quad (50)$$

Assuming that $\sigma_{cr} = f_y / \bar{\lambda}^2$ and $\chi = \sigma_b / f_y$ it is possible to express the basic form of the curve as a quadratic equation:

$$\chi^2 \cdot \bar{\lambda}^2 - \chi (1 + \eta + \bar{\lambda}^2) + 1 = 0 \quad (51)$$

By solving the equation, we can get the smallest root:

$$\chi = \frac{(1 + \eta + \bar{\lambda}^2) - \sqrt{(1 + \eta + \bar{\lambda}^2)^2 - 4\bar{\lambda}^2}}{2\bar{\lambda}^2} \quad (52)$$

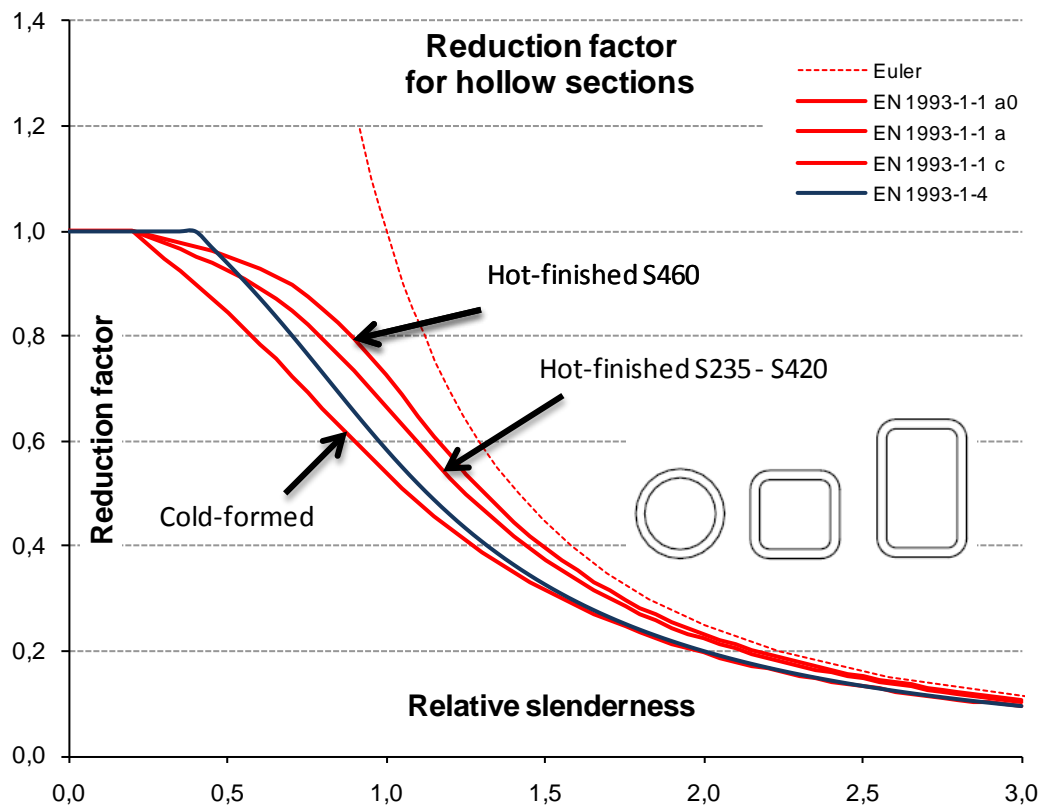
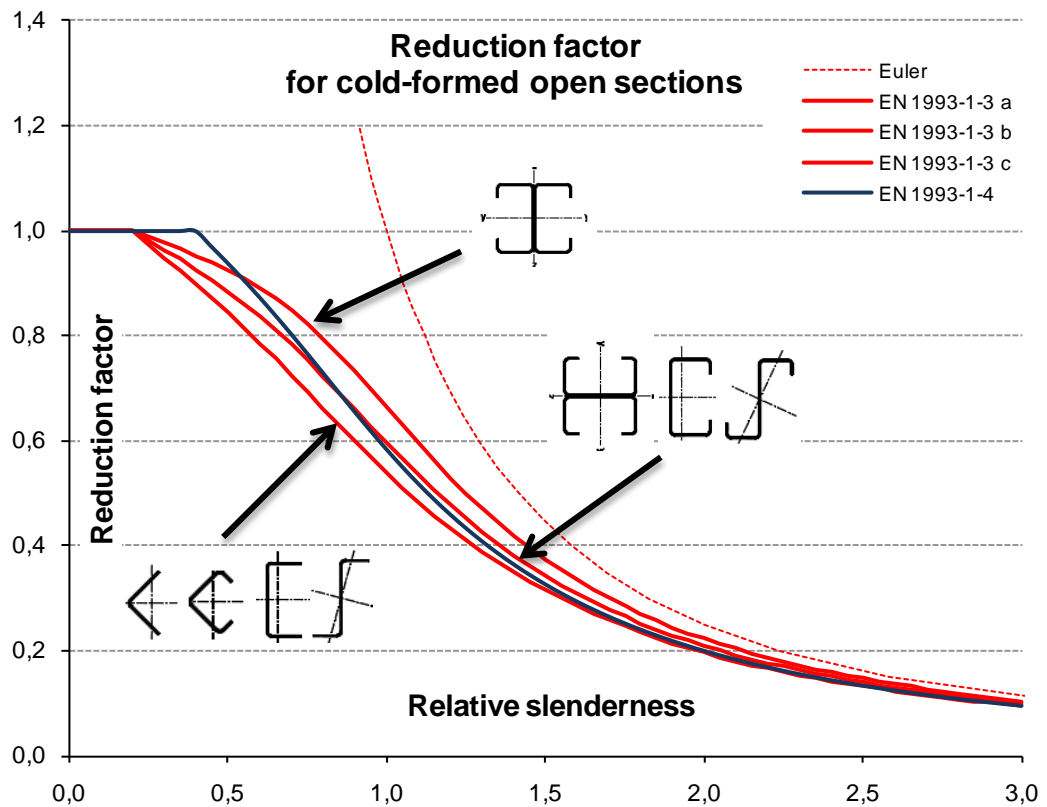
Multiplying the fraction with conjugated term $\left(1 + \eta + \bar{\lambda}^2\right) + \sqrt{\left(1 + \eta + \bar{\lambda}^2\right)^2 - 4\bar{\lambda}^2}$, it is possible to write the buckling curve in the form used in Eurocode 3 [77] and AS/NZS [35]:

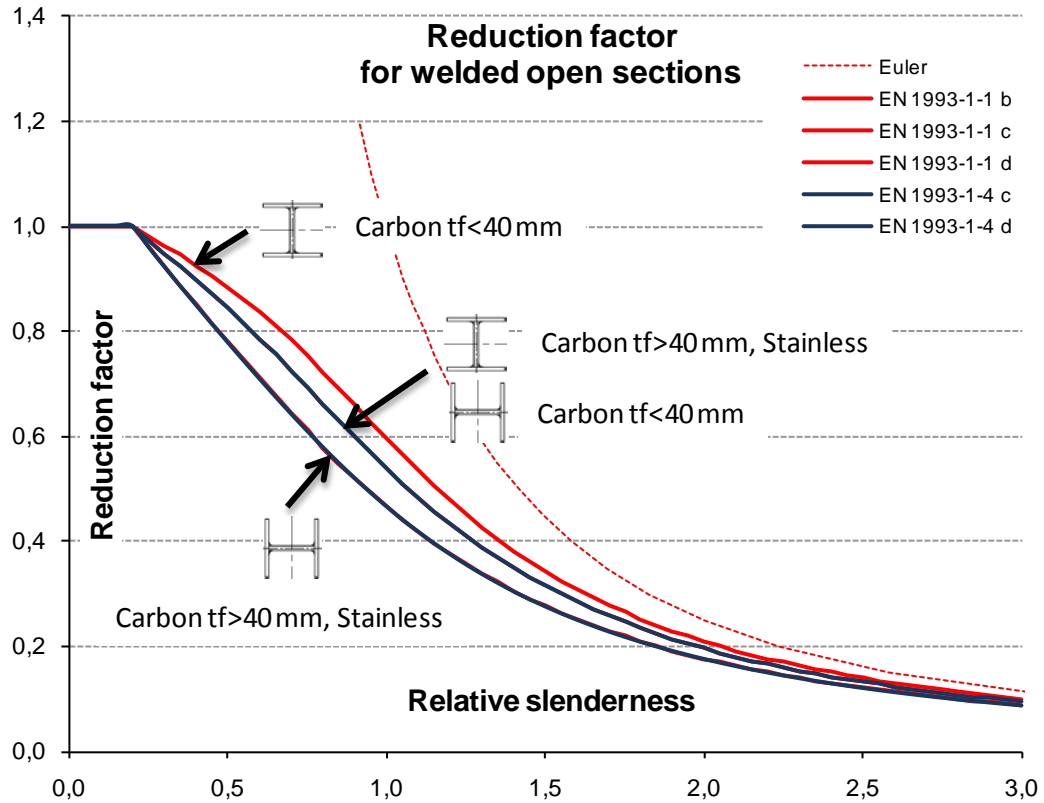
$$\chi = \frac{1}{\phi + \sqrt{\phi^2 - \bar{\lambda}^2}}, \text{ where } \phi = 0.5\left(1 + \eta + \bar{\lambda}^2\right) \text{ and } \eta = \alpha\left(\bar{\lambda} - \bar{\lambda}_0\right). \quad (53)$$

The coefficients are derived from experiments with geometrical imperfections equal to $L/1000$ assuming that $E = 210 \text{ GPa}$ and $f_y = 255 \text{ MPa}$ ($\lambda_1 = 90.15$). However, it is not possible to calculate material imperfections from the recommended equivalent imperfection table because it depends on the unknown A/W ratio which is in reality different for each cross-section. It should be also noted that yield strength f_y is section-dependent in cold-formed members because it refers to the average yield strength f_{ya} of the whole cross-section as it is defined in Eurocode 3 [1].

Table 9. Imperfection factors and the initial slenderness for carbon and stainless steel in Eurocode 3.

	α	$\bar{\lambda}_0$
Carbon steel curve a ₀	0.2	0.13
Carbon steel curve a	0.2	0.21
Carbon steel curve b, Stainless steel TB, TFB, LTB	0.2	0.34
Carbon steel curve c, Stainless steel FB of welded open sections (major axis)	0.2	0.49
Carbon steel curve d, Stainless steel FB of welded open sections (minor axis)	0.2	0.76
Stainless steel FB of cold-formed sections	0.4	0.49





9.2 Nonlinear material

Although the previous calculation assumes ideally elastic-plastic behaviour, the material nonlinearity plays an important role in the buckling behaviour, especially the nonlinear factor n of the first stage of material model. The problem is addressed for example in ASCE standards [34] disregarding initial imperfections, or by fitting the elastic-plastic material strength curves to experimental data in Eurocode and AS/NZS standards [33, 35, 97, 98]. The detailed comparison of existing standards was published by SCI (Baddoo, 2003) [99].

9.2.1 Transformation of Euler's curve

The non-linear model can be included in the theoretical strength curve by replacing constant modulus of elasticity with stress-dependent tangent modulus from Ramberg-Osgood law (15).

$$E_t = \frac{df}{d\varepsilon} = \frac{Ef_y}{f_y + 0.002nE \left(f/f_y \right)^{n-1}} \quad (54)$$

resulting in recursive model of Euler's formula [96] without initial imperfections:

$$\chi = \frac{1}{\lambda^2} \left(1 + 0.002 \frac{nE}{f_y} \chi^{n-1} \right)^{-1} \quad (55)$$

This is the common approach in ASCE [34] and the formula is mentioned also in the commentary to the Design Manual for Structural Stainless Steel [98].

The model sensitivity to variation of non-linear parameter n and yield strength f_y is demonstrated in Figure 19 and Figure 20 assuming that:

$E = 200 \text{ GPa}$, n varies from 5 to 25 and f_y varies from 300 to 500 MPa.

Typically, the curve is not very sensitive to different yield stresses (see Figure 19). On the other hand, nonlinear factor plays an important role in the curve shape, especially in lower slenderness (see Figure 20). Difference between extreme values of reduction factor is also plotted in the charts indicating that the non-linear material (with $n = 10$) has a significant influence on reduction factor at slenderness lower than 1.5.

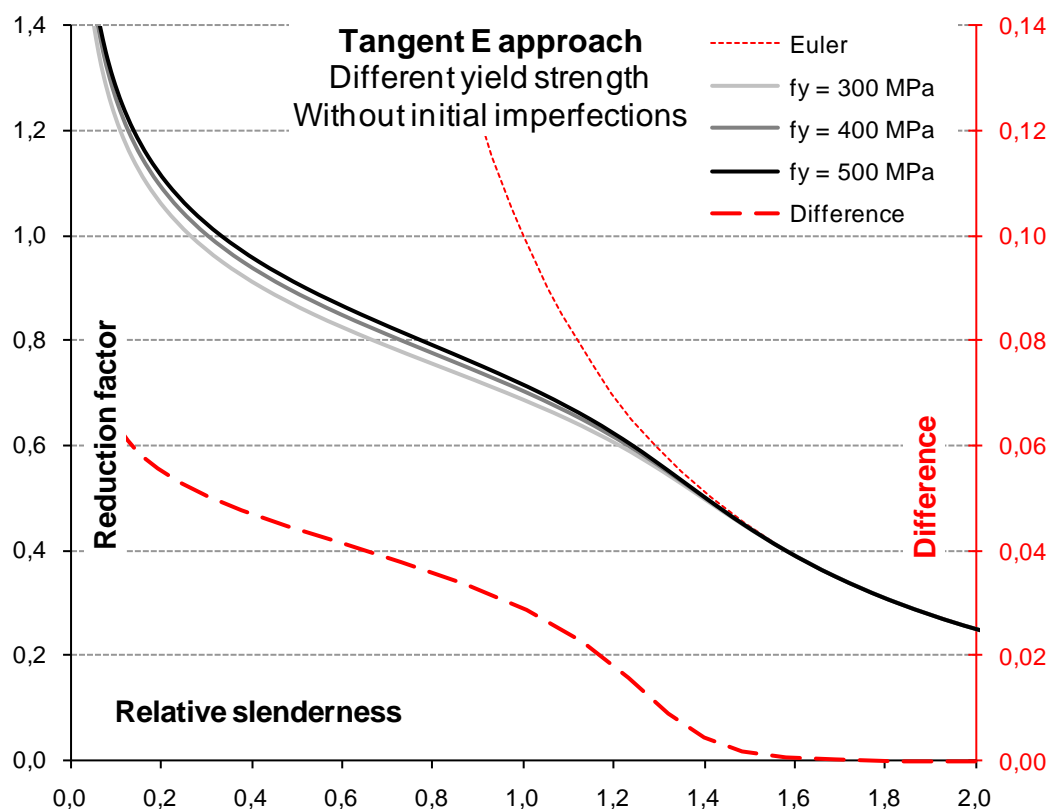


Figure 19. Transformed buckling curves with fixed $n = 10$.

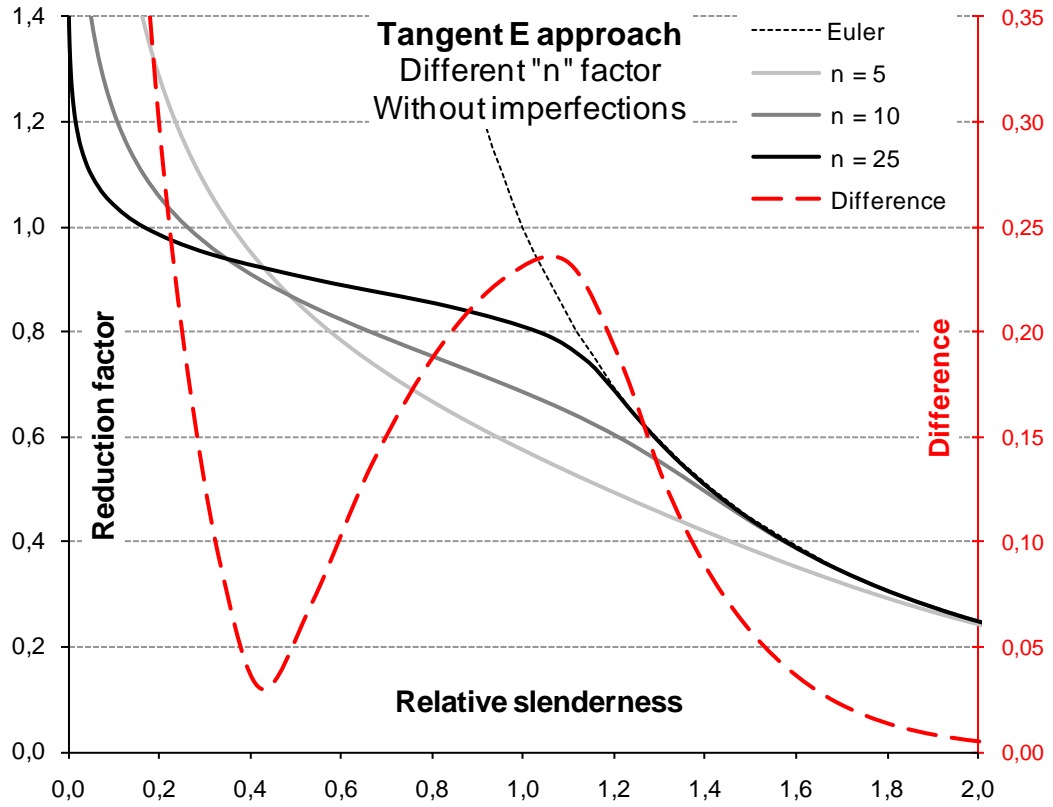


Figure 20. Transformed buckling curves with fixed $f_y = 300$ MPa.

9.2.2 Transformation of Ayrton-Perry curve

The idea of using Ayrton-Perry formula with nonlinear material was introduced by Rasmussen [81] by changing the imperfection factor n and 0.2% elastic strain e in Ramberg-Osgood model and calibrating the equation (55) with curve-fitting method.

$$\eta = \alpha \left[\left(\bar{\lambda} - \bar{\lambda}_1 \right)^\beta - \bar{\lambda}_0 \right] \geq 0, \text{ where}$$

$$\alpha = \frac{1.5}{\left(e^{0.6} + 0.03 \right) \left(n^{\left(\frac{0.0048}{e^{0.55}} \right) + 1.4} + 13 \right)} + \frac{0.002}{e^{0.6}}$$

$$\beta = \frac{0.36 \exp(-n)}{e^{0.45} + 0.007} + \tanh \left(\frac{n}{180} + \frac{6 \cdot 10^{-6}}{e^{1.4}} + 0.04 \right) \quad (56)$$

$$\bar{\lambda}_0 = 0.82 \left(\frac{e}{e + 0.0004} - 0.01n \right) \geq 0.2$$

$$\bar{\lambda}_1 = 0.8 \frac{e}{e + 0.0018} \left[1 - \left(\frac{n - 5.5}{n + \frac{6e - 0.0054}{e + 0.0015}} \right)^{1.2} \right]$$

However, the same effect could be described more clearly without need of regression analysis to fit the experimental data. Applying the transformation used in Chapter 9.2.1 to Ayrton-Perry curve (52), we can obtain recursive model that can be solved numerically (e.g. by iterative approach).

$$\bar{\lambda}^* = \bar{\lambda} \cdot \sqrt{1 + 0.002n \frac{E}{f_y} \chi^{n-1}}, \text{ where} \quad (57)$$

$$\chi = \frac{1}{\phi + \sqrt{\phi^2 - \bar{\lambda}^{*2}}}, \quad \phi = 0.5 \left(1 + \eta + \bar{\lambda}^{*2} \right), \quad \eta = \alpha \left(\bar{\lambda}^* - \bar{\lambda}_0 \right).$$

with the following limitation: $\bar{\lambda}_0^* < 1.0$, therefore $\bar{\lambda}_0 < \frac{1}{\sqrt{1 + 0.002n E/f_y}}$.

The influence of different yield strength and “n” factor is demonstrated on Figure 21 and Figure 22 assuming that:

$\alpha = 0.49$ and $\bar{\lambda}_0 = 0.2$, $E = 200 \text{ GPa}$,

n varies from 5 to 25 and f_y varies from 300 to 500 MPa.

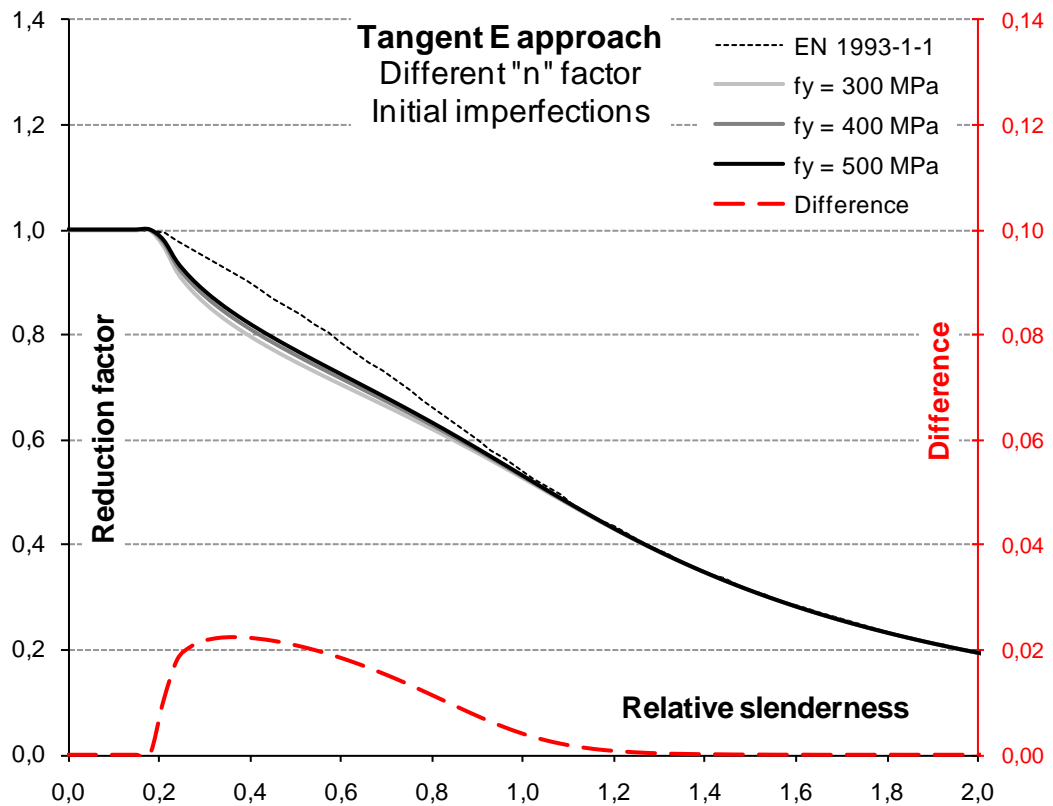


Figure 21. Non-linear material curves with fixed $n = 10$.

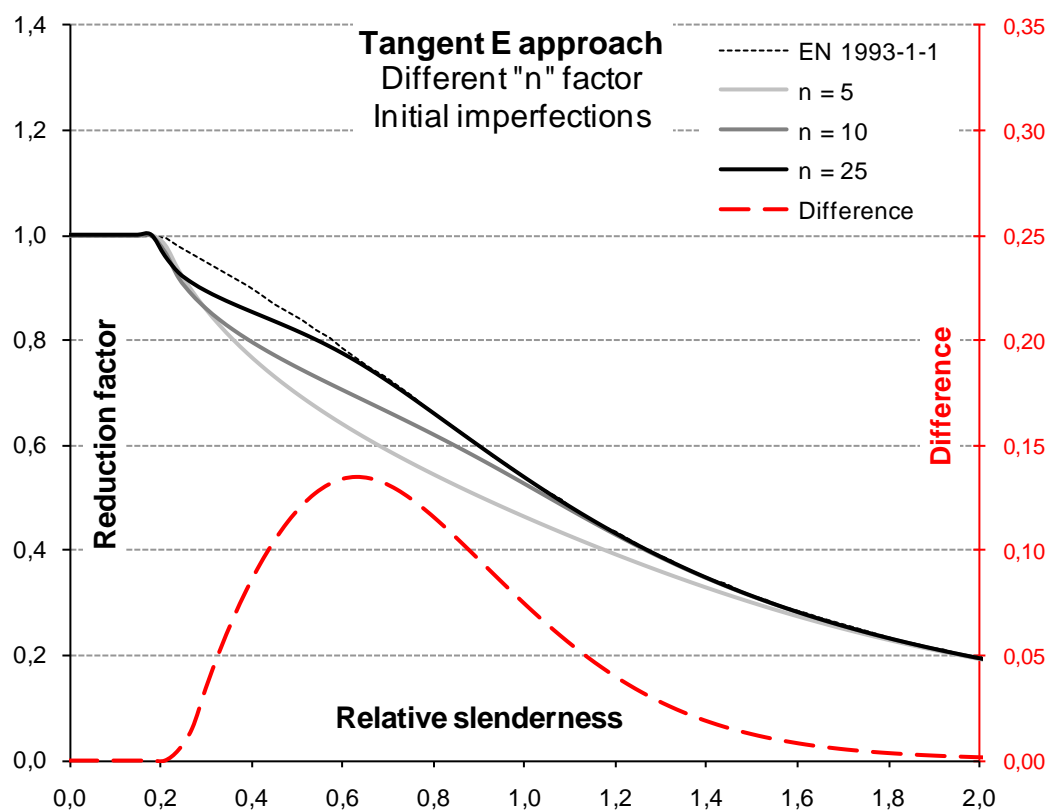


Figure 22. non-linear material curves with fixed $f_y = 300 \text{ MPa}$.

10 Numerical studies overview

In the following table the different approaches to numerical modelling of cold-formed members are summarized. Although the overview is focused on modelling of stainless steel members, few studies of carbon steel are included for comparison.

Table 10. Numerical studies overview.

Rasmussen & Rondal [100]	
University of Sydney (1997)	
Material:	Ramberg-Osgood model
Imperfections:	Sinusoidal shape with L/1500 amplitude
Res.stresses:	Included in the average material properties
Enh.properties:	
Jandera & Machacek [11]	
Czech Technical University in Prague (2000–2008)	
FE solver:	Ansys, Abaqus
Elements:	Ansys SHELL181 (4 nodes linear shell element) and Abaqus S9R5 (9 nodes quadratic thin shell element with reduced integration)
Material:	Two-stage model
Corners:	Enhanced properties for extended corners
Res.stresses:	0.63 s0,2 in 6 points (Gauss's quadratic approximation) with accompanying plastic strains
Olssen [17]	
Luleå University of Technology (2000)	
FE solver:	Abaqus
Elements:	S4R5 (4 nodes linear thin shell, reduced integration and hourglass control)
Material:	elastic-plastic with isotropic hardening
Sélen [17]	
Luleå University of Technology (2000)	
FE solver:	Abaqus
Elements:	S4 (4 nodes general shell)
Material:	Ramberg-Osgood with isotropic hardening
Imperfections:	mid-span
Res.stresses:	according to BSK 99
Stangenberg [17]	
RWTH, Aachen (2000)	
FE solver:	Marc7.3 + Mentat32
Elements:	8 nodes thick shell element with 6 degrees of freedom at each node
Imperfections:	b/800, d/500
Way [17]	
SCI, Ascot (2000)	
FE solver:	Lusas 13.1
Elements:	8 nodes thin shell element with 3 dof at corners and 5 dof at mid-nodes
Material:	elastic-plastic with isotropic hardening

Imperfections:	sinusoidal, amplification from measurements
Ashraf et al. [74]	
Imperial College (2006)	
FE solver:	Abaqus
Method:	Modified Riks
Elements:	S9R5 (9 nodes quadratic thin shell element with reduced integration)
Corners:	Enhanced properties
Gardner [10]	
Imperial College (2004)	
FE solver:	Abaqus
Elements:	S9R5 (9 nodes quadratic thin shell element with reduced integration)
Imperfections:	L/2000
Res.stresses :	f_y (tension) on central portion of plate B/5 and $f_y/4$ on the rest
Gozzi [10]	
Luleå University of Technology (2004)	
FE solver:	Abaqus
Elements:	S4R (4 nodes linear general shell, reduced integration and hourglass control)
Ellobody & Young [72]	
Tanta University, University of Hong Kong (2004)	
FE solver:	Abaqus
Method:	Riks
Elements:	S4R (4 nodes linear general shell, reduced integration and hourglass control)
Mesh size:	10 x 20 mm
Test:	Stub column test with fixed rotation on SHS, RHS profiles
Imperfections:	Local and overall in long columns, only local in short columns
Macdonald & Rhodes [5]	
Glasgow Caledonian University (2007)	
FE solver:	Ansys
Elements:	SHELL181 (4 nodes linear general shell element)
Material:	Ramberg-Osgood
Test:	Flexural buckling test on lipped channels
Imperfections:	Mid-span imperfection
Lecce & Rasmussen [63]	
University of Sydney (2006)	
FE solver:	Abaqus
Elements:	S4R (4 nodes linear general shell, reduced integration and hourglass control)
Material:	Anisotropic Ramberg-Osgood
Test:	Stub column test with fixed rotation
Corners:	Enhanced properties
Imperfections:	Mid-span imperfection
Schafer [68]	
Johns Hopkins University, Baltimore (2008)	
FE solver:	Abaqus
Elements:	S9R5 (9 nodes quadratic thin shell element with reduced

	integration)
Material:	Anisotropic Ramberg-Osgood
Test:	Stub column test with fixed rotation
Corners:	Enhanced properties
Imperfections:	Mid-span imperfection
Greinier [75]	
Technical University in Graz (2008)	
FE solver:	Abaqus
Elements:	B31OS (open-section beam incl. warping), B31 (general beam)
Material:	Two-stage model
Imperfections:	L/1000 in major axis (in-plane FB), both axes (out-of-plane FB), minor axis (LTB)
Res.stresses	only from welding (IPE welded section)
Res.strains	10% over the corss-section thickness up to 3t from corners
Theofanous	
Imperial College (2010)	
FE solver:	Abaqus
Elements:	S4R (4 nodes linear general shell, reduced integration and hourglass control)
Material	Gardner's model
Res. stresses:	Included in material model
Corners:	Enhanced properties

References

- [1] European Committee for Standardization Eurocode 3. Design of steel structures. Part 1-3: General rules. Supplementary rules for coldformed members and sheeting. Brussels, Belgium: 2006.
- [2] Rasmussen, K.J.R. & Hancock, G.J. Design of Cold-Formed Stainless Steel Tubular Members. I: Columns. *Journal of Structural Engineering* 1993, August 1993, Vol. 119, No. 8, pp. 2349–2367. doi: 10.1061/(ASCE)0733-9445(1993)119:8(2349).
- [3] VTT Research Notes 1619. Talja, A. & Salmi, P. Design of stainless steel RHS beams, columns and beam-columns. Espoo, Finland: VTT Technical Research Centre of Finland, 1995.
- [4] Gardner, L. & Nethercot, D.A. Experiments on stainless steel hollow sections – Part 2: Member behaviour of columns and beams. *Journal of Constructional Steel Research* 2004, 9, Vol. 60, No. 9, pp. 1319–1332. ISSN 0143-974X. doi: DOI: 10.1016/j.jcsr.2003.11.007.
- [5] Macdonald, M., Rhodes, J. & Kotelko, M. Stainless steel stub columns subject to combined bending and axial loading. *Thin-Walled Structures* 2007, 11, Vol. 45, No. 10-11, pp. 893–897. ISSN 0263-8231. doi: DOI: 10.1016/j.tws.2007.08.044.
- [6] Becque, J. & Rasmussen, K.J.R. Experimental investigation of local-overall interaction buckling of stainless steel lipped channel columns. *Journal of Constructional Steel Research* 2009, 9, Vol. 65, No. 8–9, pp. 1677–1684. ISSN 0143-974X. doi: DOI: 10.1016/j.jcsr.2009.04.025.
- [7] Young, B. & Hartono, W. Compression Tests of Stainless Steel Tubular Members. *Journal of Structural Engineering* 2002, June 2002, Vol. 128, No. 6, pp. 754–761. doi: 10.1061/(ASCE)0733-9445(2002)128:6(754).
- [8] Young, B. & Liu, Y. Experimental Investigation of Cold-Formed Stainless Steel Columns. *Journal of Structural Engineering* 2003, February 2003, Vol. 129, No. 2, pp. 169–176. doi: 10.1061/(ASCE)0733-9445(2003)129:2(169).
- [9] Liu, Y. & Young, B. Buckling of stainless steel square hollow section compression members. *Journal of Constructional Steel Research* 2003, 2, Vol. 59, No. 2, pp. 165–177. ISSN 0143-974X. doi: DOI: 10.1016/S0143-974X(02)00031-7.
- [10] Baddoo, N., Chinen, V.L., Gozzi, J., Clarin, M., Conrad, F., Talja, A., Ala-Outinen, T., Viherma, R., Nilimaa, H., Gardner, L., Zili, G., Riscifuli, S., Fattorini, F., Kasper, R., Stangenberg, H., Blanguernon, A. & Zhao, B. Structural design of cold worked austenitic stainless steel. Brussels: European Commission, 2004.
- [11] Jandera, M., Gardner, L. & Machacek, J. Residual stresses in cold-rolled stainless steel hollow sections. *Journal of Constructional Steel Research* 2008, 11, Vol. 64, No. 11, pp. 1255–1263. ISSN 0143-974X. doi: DOI: 10.1016/j.jcsr.2008.07.022.

- [12] Gardner, L. & Nethercot, D.A. Experiments on stainless steel hollow sections–Part 1: Material and cross-sectional behaviour. *Journal of Constructional Steel Research* 2004, 9, Vol. 60, No. 9, pp. 1291–1318. ISSN 0143-974X. doi: DOI: 10.1016/j.jcsr.2003.11.006.
- [13] Gardner, L. & Nethercot, D.A. Numerical Modeling of Stainless Steel Structural Components – A Consistent Approach. *Journal of Structural Engineering* 2004, October 2004, Vol. 130, No. 10, pp. 1586–1601. doi: 10.1061/(ASCE)0733-9445(2004)130:10(1586).
- [14] Theofanous, M., Chan, T.M. & Gardner, L. Flexural behaviour of stainless steel oval hollow sections. *Thin-Walled Structures* 2009, 7, Vol. 47, No. 6–7, pp. 776–787. ISSN 0263-8231. doi: DOI: 10.1016/j.tws.2009.01.001.
- [15] Theofanous, M., Chan, T.M. & Gardner, L. Structural response of stainless steel oval hollow section compression members. *Engineering Structures* 2009, 4, Vol. 31, No. 4, pp. 922–934. ISSN 0141-0296. doi: DOI: 10.1016/j.engstruct.2008.12.002.
- [16] Theofanous, M. & Gardner, L. Experimental and numerical studies of lean duplex stainless steel beams. *Journal of Constructional Steel Research* 2010, 6, Vol. 66, No. 6, pp. 816–825. ISSN 0143-974X. doi: DOI: 10.1016/j.jcsr.2010.01.012.
- [17] Burgan, B.A., Baddoo, N., Gardner, L., Way, J., Johansson, B., Olssen, A., Selen, E., Viherma, R., Kouhi, J., Talja, A., Lihavainen, V.M., Niemi, E., Ryan, I., Zhao, B., Stangenberg, H., Barteri, M., Budano, S. & Riscifuli, S. Development of the use of stainless steel in construction. Brussels: European Commission, 2000.
- [18] Korvink, S.A., van den Berg, G.J. & van der Merwe, P. Web crippling of stainless steel cold-formed beams. *Journal of Constructional Steel Research* 1995, Vol. 34, No. 2–3, pp. 225–248. ISSN 0143-974X. doi: DOI: 10.1016/0143-974X(94)00026-E.
- [19] Bredenkamp, P.J. & van den Berg, G.J. The strength of stainless steel built-up I-section columns. *Journal of Constructional Steel Research* 1995, Vol. 34, No. 2–3, pp. 131–144. ISSN 0143-974X. doi: DOI: 10.1016/0143-974X(94)00023-B.
- [20] Zhou, F. & Young, B. Cold-Formed Stainless Steel Sections Subjected to Web Crippling. *Journal of Structural Engineering* 2006, 01, Vol. 132, No. 1, pp. 134–144. ISSN 07339445. doi: 10.1061/(ASCE)0733-9445(2006)132:1(134).
- [21] Zhou, F. & Young, B. Experimental and numerical investigations of cold-formed stainless steel tubular sections subjected to concentrated bearing load. *Journal of Constructional Steel Research* 2007, 11, Vol. 63, No. 11, pp. 1452–1466. ISSN 0143-974X. doi: DOI: 10.1016/j.jcsr.2006.12.007.
- [22] Zhou, F. & Young, B. Experimental Investigation of Cold-Formed High-Strength Stainless Steel Tubular Members Subjected to Combined Bending and Web Crippling. *Journal of Structural Engineering* 2007, 07, Vol. 133,

No. 7, pp. 1027–1034. ISSN 07339445. doi: 10.1061/(ASCE)0733-9445(2007)133:7(1027).

- [23] Zhou, F. & Young, B. Cold-Formed High-Strength Stainless Steel Tubular Sections Subjected to Web Crippling. *Journal of Structural Engineering* 2007, 03, Vol. 133, No. 3, pp. 368–377. ISSN 07339445. doi: 10.1061/(ASCE)0733-9445(2007)133:3(368).
- [24] Zhou, F. & Young, B. Web Crippling of Cold-Formed Stainless Steel Tubular Sections. *Advances in Structural Engineering* 2008, 12, Vol. 11, No. 6, pp. 679–691. ISSN 13694332.
- [25] Zhou, F. & Young, B. Tests of cold-formed stainless steel tubular flexural members. *Thin-Walled Structures* 2005, 9, Vol. 43, No. 9, pp. 1325–1337. ISSN 0263-8231. doi: DOI: 10.1016/j.tws.2005.06.005.
- [26] Rossi, B., Jaspart, J. & Rasmussen, K.J.R. Combined Distortional and Overall Flexural-Torsional Buckling of Cold-Formed Stainless Steel Sections: Experimental Investigations. *Journal of Structural Engineering* 2010, April 2010, Vol. 136, No. 4, pp. 354–360. doi: 10.1061/(ASCE)ST.1943-541X.0000130.
- [27] Mirambell, E. & Real, E. On the calculation of deflections in structural stainless steel beams: an experimental and numerical investigation. *Journal of Constructional Steel Research* 2000, 4, Vol. 54, No. 1, pp. 109–133. ISSN 0143-974X. doi: DOI: 10.1016/S0143-974X(99)00051-6.
- [28] Rasmussen, K.J.R. & Hancock, G.J. Design of Cold-Formed Stainless Steel Tubular Members. II: Beams. *Journal of Structural Engineering* 1993, August 1993, Vol. 119, No. 8, pp. 2368–2386. doi: 10.1061/(ASCE)0733-9445(1993)119:8(2368).
- [29] Rasmussen, K.J.R., Burns, T., Bezkorovainy, P. & Bambach, M.R. Numerical modelling of stainless steel plates in compression. *Journal of Constructional Steel Research* 2003, 11, Vol. 59, No. 11, pp. 1345–1362. ISSN 0143-974X. doi: DOI: 10.1016/S0143-974X(03)00086-5.
- [30] Becque, J. & Rasmussen, K.J.R. Experimental Investigation of the Interaction of Local and Overall Buckling of Stainless Steel I-Columns. *Journal of Structural Engineering* 2009, November 2009, Vol. 135, No. 11, pp. 1340–1348. doi: 10.1061/(ASCE)ST.1943-541X.0000051.
- [31] Bardi, F.C. & Kyriakides, S. Plastic buckling of circular tubes under axial compression—part I: Experiments. *International Journal of Mechanical Sciences* 2006, 8, Vol. 48, No. 8, pp. 830–841. ISSN 0020-7403. doi: DOI: 10.1016/j.ijmecsci.2006.03.005.
- [32] Kaitila, O. Web crippling of cold-formed thin-walled steel cassettes. Espoo, Finland: Helsinki University of Technology, 2004.
- [33] European Committee for Standardization Eurocode 3. Design of steel structures. Part 1-4: General rules. Supplementary rules for stainless steels. Brussels, Belgium: 2006.

- [34] American Society of Civil Engineers & Structural Engineering Institute Specification for the Design of Cold-Formed Stainless Steel Structural Members. Reston, Virginia: 2002. ISBN 0-7844-0556-5.
- [35] Standards Australia & Standards New Zealand Australian/New Zealand Standard: Cold-formed stainless steel structures. Sydney Australia: 2001. ISBN 0 7337 3979 2.
- [36] Bakker, M.C.M. Web crippling of cold-formed steel members. The Netherlands: Eindhoven University of Technology, 1992.
- [37] Hofmeyer, H. Combined Web Crippling and Bending Moment Failure of First-Generation Trapezoidal Steel Sheeting: Experiment, Finite Element Models, Mechanical models. The Netherlands: Eindhoven University of Technology, 2000.
- [38] Rhodes, J. & Nash, D. An investigation of web crushing behaviour in thin-walled beams. Thin-Walled Structures 1998, 9, Vol. 32, No. 1-3, pp. 207–230. ISSN 0263-8231. doi: DOI: 10.1016/S0263-8231(98)00035-4.
- [39] Winter, G. & Pian, R.H.J. Crushing strength of thin steel webs. Cornell Bulletin 1946, pp. 35.
- [40] Baehre, R. Sheet metal panels for use in building construction – recent research projects in Sweden. 3rd international specialty conference on cold-formed steel structures. 1975. 1975.
- [41] Final report, civil engineering study, 784. Hetrakul, N. & Yu, W.W. Structural behaviour of beam webs subjected to web crippling and a combination of web crippling and bending. Rolla (MO): University of Missouri-Rolla, 1978.
- [42] Civil engineering study 81-2, structural series. Yu, W.W. Web crippling and combined web crippling and bending of steel decks. Rolla (MO): University of Missouri-Rolla, 1981.
- [43] Studnicka, J. Web crippling of wide deck sections. In: Anonymous Recent research and developments in cold-formed steel design and construction. Rolla (MO): Department of Civil Engineering. University of Missouri-Rolla., 1991. Pp. 317–334.
- [44] Gerges, R.R. Web crippling of single web cold formed steel members subjected to End One-Flange loading. Waterloo (ON, Canada): University of Waterloo, 1997.
- [45] Avci, O. & Easterling, W.S. Web crippling strength of multi-web steel deck sections subjected to End One-Flange loading. Blacksburg (VA, USA): Virginia Polytechnic Institute and State University, 2002.
- [46] Wing, B.A. Web crippling and the interaction of bending and web crippling of unreinforced multi-web cold-formed steel sections. Waterloo (ON, Canada): University of Waterloo, 1981.

- [47] Santaputra, C., Parks, M.B. & Yu, W.W. Web crippling strength of high strength steel beams. 8th International Specialty Conference on Cold-Formed Steel Structures. 1986. St. Louis, Missouri, USA: 1986.
- [48] Young, B. & Hancock, G.J. Cold-Formed Steel Channels Subjected to Concentrated Bearing Load. *Journal of Structural Engineering* 2003, 08, Vol. 129, No. 8, pp. 1003. ISSN 07339445.
- [49] Zhao, X. & Hancock, G.J. Square and Rectangular Hollow Sections under Transverse End-Bearing Force. *Journal of Structural Engineering* 1995, 09, Vol. 121, No. 9, pp. 1323. ISSN 07339445.
- [50] Bähr, G. Eine einfache Abschätzung der aufnehmbaren Endauflagerkräfte von Stahl-Trapezblechprofilen. *Die Bautechnik* 1978, No. 11, pp. 388–390.
- [51] Reinsch, W. Das Kantenbeulen zur rechnerischen Ermittlung von Stahltrapezblechträger. Germany: Technische Hochschule Darmstadt, 1983.
- [52] Tsai, Y.M. & Crisinel, M. Moment redistribution in continuous profiled sheeting, thin-walled metal structures in buildings. *IABSE proceedings*, vol. 49. Zürich: 1946. P. 107.
- [53] Vaessen, M.J. On the elastic web crippling stiffness of thin-walled cold-formed steel members. The Netherlands: Department of Structural Design, Eindhoven University of Technology, 1995.
- [54] Hofmeyer, H., Kerstens, J.G.M., Snijder, H.H. & Bakker, M.C.M. New prediction model for failure of steel sheeting subject to concentrated load (web crippling) and bending. *Thin-Walled Structures* 2001, 9, Vol. 39, No. 9, pp. 773–796. ISSN 0263-8231. doi: DOI: 10.1016/S0263-8231(01)00032-5.
- [55] Hofmeyer, H., Kerstens, J.G.M., Snijder, H.H. & Bakker, M.C.M. Research on the behaviour of combined web crippling and bending of steel deck sections. 13th International Speciality Conference on Cold-formed Steel Structures. St. Louis, Missouri (USA): 1996.
- [56] Hofmeyer, H. Cross-section crushing behaviour of hat-sections (Part I: Numerical modelling). *Thin-Walled Structures* 2005, 8, Vol. 43, No. 8, pp. 1143–1154. ISSN 0263-8231. doi: DOI: 10.1016/j.tws.2005.03.009.
- [57] American Iron and Steel Institute Specification for the design of Cold-Formed Steel Structural Members with Commentary. 1986.
- [58] Zhou, F. & Young, B. Yield line mechanism analysis on web crippling of cold-formed stainless steel tubular sections under two-flange loading. *Engineering Structures* 2006, 5, Vol. 28, No. 6, pp. 880–892. ISSN 0141-0296. doi: DOI: 10.1016/j.engstruct.2005.10.021.
- [59] Von-Karman, T., Sechler, E.E. & Donnell, L.H. The strength of thin plates in compression. *Transactions, ASME* 1932, No. 54, p. 53.

- [60] Ashraf, M., Gardner, L. & Nethercot, D.A. Structural Stainless Steel Design: Resistance Based on Deformation Capacity. *Journal of Structural Engineering* 2008, 03, Vol. 134, No. 3, pp. 402–411. ISSN 07339445. doi: 10.1061/(ASCE)0733-9445(2008)134:3(402).
- [61] Gardner, L. The Continuous Strength Method. *Proceedings of the Institution of Civil Engineers. Structures and Buildings*. 161 (SB3) 2008. 2008. P. 127.
- [62] Schafer, B.W. Review: The Direct Strength Method of cold-formed steel member design. *Journal of Constructional Steel Research* 2008, 8, Vol. 64, No. 7–8, pp. 766–778. ISSN 0143-974X. doi: DOI: 10.1016/j.jcsr.2008.01.022.
- [66] Silvestre, N. & Camotim, D. Distortional buckling formulae for cold-formed steel C- and Z-section members: Part II – Validation and application. *Thin-Walled Structures* 2004, 11, Vol. 42, No. 11, pp. 1599–1629. ISSN 0263-8231. doi: DOI: 10.1016/j.tws.2004.05.002.
- [67] Ungureanu, V. & Dubina, D. Recent research advances on ECBL approach.: Part I: Plastic–elastic interactive buckling of cold-formed steel sections. *Thin-Walled Structures* 2004, 2, Vol. 42, No. 2, pp. 177–194. ISSN 0263-8231. doi: DOI: 10.1016/S0263-8231(03)00056-9.
- [68] Schafer, B.W. & Peköz, T. Computational modeling of cold-formed steel: characterizing geometric imperfections and residual stresses. *Journal of Constructional Steel Research* 1998, 9, Vol. 47, No. 3, pp. 193–210. ISSN 0143-974X. doi: DOI: 10.1016/S0143-974X(98)00007-8.
- [69] European Committee for Standardization Eurocode 3. Design of steel structures. Part 1-5: Plated structural elements. Brussels, Belgium: 2006.
- [70] Hibbit, Karlsson, Sorenson & Pawtucket ABAQUS user's manual version 6.8.2009.
- [71] Ádány, S. & Schafer, B.W. A full modal decomposition of thin-walled, single-branched open cross-section members via the constrained finite strip method. *Journal of Constructional Steel Research* 2008, 1, Vol. 64, No. 1, pp. 12–29. ISSN 0143-974X. doi: DOI: 10.1016/j.jcsr.2007.04.004.
- [72] Ellobody, E. & Young, B. Structural performance of cold-formed high strength stainless steel columns. *Journal of Constructional Steel Research* 2005, 12, Vol. 61, No. 12, pp. 1631–1649. ISSN 0143-974X. doi: DOI: 10.1016/j.jcsr.2005.05.001.
- [73] Rossi, B., Jaspart, J. & Rasmussen, K.J.R. Combined Distortional and Overall Flexural-Torsional Buckling of Cold-Formed Stainless Steel Sections: Design. *Journal of Structural Engineering* 2010, April 2010, Vol. 136, No. 4, pp. 361–369. doi: 10.1061/(ASCE)ST.1943-541X.0000147.
- [74] Ashraf, M., Gardner, L. & Nethercot, D.A. Finite element modelling of structural stainless steel cross-sections. *Thin-Walled Structures* 2006, 10, Vol. 44, No. 10, pp. 1048–1062. ISSN 0263-8231. doi: DOI: 10.1016/j.tws.2006.10.010.

- [75] Greiner, R. & Kettler, M. Interaction of bending and axial compression of stainless steel members. *Journal of Constructional Steel Research* 2008, 11, Vol. 64, No. 11, pp. 1217–1224. ISSN 0143-974X. doi: DOI: 10.1016/j.jcsr.2008.05.008.
- [76] Zhang, L. & Tong, G.S. Lateral buckling of web-tapered I-beams: A new theory. *Journal of Constructional Steel Research* 2008, 12, Vol. 64, No. 12, pp. 1379–1393. ISSN 0143-974X. doi: DOI: 10.1016/j.jcsr.2008.01.014.
- [77] European Committee for Standardization Eurocode 3: Design of steel structures. Part 1-1: General rules and rules for buildings. Brussels, Belgium: 2005.
- [78] Holmquist, J.L. & Nadai, A. A theoretical and experimental approach to the problem of collapse of deep-well casing. *Drilling and Production Practice* 1939, pp. 392–420.
- [79] Technical Note No. 902. Ramberg, W. & Osgood, W.R. Description of stress-strain curves by three parameters. Washington, D.C., USA: National Advisory Committee for Aeronautics, 1943.
- [80] Technical Note No. 927. Hill, H.N. Determination of stress-strain relations from "offset" yield strength values. Washington, D.C., USA: National Advisory Committee for Aeronautics, 1944.
- [81] Rasmussen, K.J.R. Full-range stress-strain curves for stainless steel alloys. *Journal of Constructional Steel Research* 2003, 1, Vol. 59, No. 1, pp. 47–61. ISSN 0143-974X. doi: DOI: 10.1016/S0143-974X(02)00018-4.
- [82] Gardner, L. & Ashraf, M. Structural design for non-linear metallic materials. *Engineering Structures* 2006, 5, Vol. 28, No. 6, pp. 926–934. ISSN 0141-0296. doi: DOI: 10.1016/j.engstruct.2005.11.001.
- [83] Quach, W.M., Teng, J.G. & Chung, K.F. Three-Stage Full-Range Stress-Strain Model for Stainless Steels. *Journal of Structural Engineering* 2008, September 2008, Vol. 134, No. 9, pp. 1518–1527. doi: 10.1061/(ASCE)0733-9445(2008)134:9(1518).
- [84] European Committee for Standardization EN 10088-2: Stainless steels – Part 2: Technical delivery conditions for sheet/plate and strip of corrosion resisting steels for general purposes. Brussels, Belgium: 2005.
- [85] Abdella, K. An explicit stress formulation for stainless steel applicable in tension and compression. *Journal of Constructional Steel Research* 2007, 3, Vol. 63, No. 3, pp. 326–331. ISSN 0143-974X. doi: DOI: 10.1016/j.jcsr.2006.06.001.
- [86] Abdella, K. Explicit full-range stress–strain relations for stainless steel at high temperatures. *Journal of Constructional Steel Research* 2009, 4, Vol. 65, No. 4, pp. 794–800. ISSN 0143-974X. doi: DOI: 10.1016/j.jcsr.2008.09.001.

- [87] Rossi, B. Mechanical behavior of ferritic grade 3Cr12 stainless steel – Part 1: Experimental investigations. *Thin-Walled Structures* 2010, 7, Vol. 48, No. 7, pp. 553–560. ISSN 0263-8231. doi: DOI: 10.1016/j.tws.2010.02.008.
- [88] Rossi, B. Mechanical behavior of ferritic grade 3Cr12 stainless steel – Part 2: Yield locus and hardening laws. *Thin-Walled Structures* 2010, 7, Vol. 48, No. 7, pp. 540–552. ISSN 0263-8231. doi: DOI: 10.1016/j.tws.2010.02.007.
- [89] Karren, K.W. Corner Properties of Cold-formed Steel Shapes. *Journal of the Structural Division* 1967, Vol. 93, No. ST1, pp. 401–432.
- [90] Ashraf, M., Gardner, L. & Nethercot, D.A. Strength enhancement of the corner regions of stainless steel cross-sections. *Journal of Constructional Steel Research* 2005, 1, Vol. 61, No. 1, pp. 37–52. ISSN 0143-974X. doi: DOI: 10.1016/j.jcsr.2004.06.001.
- [91] Cruise, R.B. & Gardner, L. Strength enhancements induced during cold forming of stainless steel sections. *Journal of Constructional Steel Research* 2008, 11, Vol. 64, No. 11, pp. 1310–1316. ISSN 0143-974X. doi: DOI: 10.1016/j.jcsr.2008.04.014.
- [92] Rossi, B., Degée, H. & Pascon, F. Enhanced mechanical properties after cold process of fabrication of non-linear metallic profiles. *Thin-Walled Structures* 2009, 12, Vol. 47, No. 12, pp. 1575–1589. ISSN 0263-8231. doi: DOI: 10.1016/j.tws.2009.05.004.
- [93] Abdel-Rahman, N. & Sivakumaran, K.S. Material properties models for analysis of cold-formed steel members. *Journal of Structural Engineering* 1997, 09, Vol. 123, No. 9, pp. 1135. ISSN 07339445.
- [94] Gardner, L. & Cruise, R.B. Modeling of Residual Stresses in Structural Stainless Steel Sections. *Journal of Structural Engineering* 2009, 01, Vol. 135, No. 1, pp. 42–53. ISSN 07339445. doi: 10.1061/(ASCE)0733-9445(2009)135:1(42).
- [95] Weng, C.C. & Peköz, T. Residual Stresses in Cold-Formed Steel Members. *Journal of Structural Engineering* 1990, June 1990, Vol. 116, No. 6, pp. 1611–1625. ISSN 0733-9445.
- [96] Euler, L. *Methodus inveniendi lineas curvas maximi minimive proprietate gaudentes, sive solutio problematis isoperimetrici latissimo sensu accepti*. Laussanae et Genevae: Apud Marcum-Michaelum, Bousquet & Socios, 1744.
- [97] Euro Inox and The Steel Construction Institute Design Manual For Structural Stainless Steel. 3rd ed. Euro Inox, 2006. ISBN 2-87997-204-3.
- [98] Euro Inox and The Steel Construction Institute Design Manual For Structural Stainless Steel - Commentary. 3rd ed. Euro Inox, 2007.
- [99] Baddoo, N. A comparison of stainless steel design standards. ISSF publications 2003, [Online], pp. 11.1.2011. Available from:

<http://www.worldstainless.org/NR/rdonlyres/0254E2DE-9B16-4575-BE1F-AAA596F29DE1/2462/Acomparisonofstructuralstainlesssteeldesignstandar.pdf>.

- [100] Rasmussen, K.J.R. & Rondal, J. Strength curves for metal columns. Journal of Structural Engineering 1997, 06, Vol. 123, No. 6, pp. 721. ISSN 07339445.